JOURNAL OF BACTERIOLOGY, May 1977, p. 911-936

Vol. 130, No. 2
Printed in U.S.A.

# Polysaccharide Capsule of *Escherichia coli*: Microscope Study of Its Size, Structure, and Sites of Synthesis

MANFRED E. BAYER* AND HORST THUROW

*The Institute for Cancer Research, The Fox Chase Cancer Center, Philadelphia, Pennsylvania 19111*

Received for publication 1 November 1976

This report describes the structure, size, and shape of the uncollapsed polysaccharide capsule of *Escherichia coli* strain Bi 161/42 [O9:K29(A):H$^-$], its ultrastructural preservation as well as the filamentous components of the isolated capsular material. In a temperature-sensitive mutant, sites were localized at which capsular polysaccharide is "exported" to the cell surface. The highly hydrated capsule of the wild-type cells was visible in the uncollapsed state after freeze-etching, whereas dehydration in ≥50% acetone or alcohol caused the capsule to collapse into thick bundles. This was prevented by pretreatment of the cell with capsule-specific immunoglobulin G; the capsule appeared as a homogeneous layer of 250- to 300-nm thickness. The structural preservation depended on the concentration of the anti-capsular immunoglobulin G. Temperature-sensitive mutants, unable to produce capsular antigen at elevated temperatures, showed, 10 to 15 min after shift down to permissive temperature, polysaccharide strands with K29 specificity appearing at the cell surface at roughly 20 sites per cell; concomitantly, capsule-directed antibody started to agglutinate the bacteria. The sites at which the new antigen emerged were found in random distribution over the entire surface of the organism. Spreading of purified polysaccharide was achieved on air-water interfaces; after subsequent shadow casting with heavy metal, filamentous elements were observed with a smallest class of filaments measuring 250 nm in length and 3 to 6 nm in width. At one end these fibers revealed a knoblike structure of about 10-nm diameter. The slimelike polysaccharides from mutants produced filamentous bundles of >100-$\mu$m length, with antigenic and phage-receptor properties indistinguishable from those of the wild-type K29 capsule antigen.

The bacterial capsule represents an organelle localized outside the outer membrane of the cell, thus increasing the overall dimensions of the organism. The capsule of most gram-negative bacteria is composed of hydrophilic polysaccharides carrying negative charges (39). A large number of serologically distinct capsule types have been recognized on the basis of their respective antigenic determinants (31). The bacterial capsule is involved in a variety of functions, such as cementing freshwater bacteria together (7) to form large films (28) or facilitating adhesion of marine bacteria to solid surfaces (18); furthermore, capsulated cells seem to be protected from adverse environmental conditions (12). Capsulated cells are also found in the oral flora (29), with polysaccharides serving as aggregation substances (32) and possibly playing a role in dental plaque and caries (20). Of special significance to our work is that the capsule hinders the attack by bacteriophages specific for O-antigens and lipopolysaccharides; it also protects the cells from phagocytosis by macrophages (39).

In the light microscope, the capsule may be visualized after India ink staining as a transparent "halo," owing to its impermeability to the carbon particles of the ink. Interaction with capsule-specific immune sera produces the classical "quellungs reaction" (46); in this reaction, the capsular elements interact with the antibody molecules, thus making the highly hydrated capsular material more refractile in the light microscope by the added density (contrast) of the antibody/polysaccharide complex. The reaction was described as early as 1896 in pathogenic fungi that develop an extracellular hyaline mass after exposure to a serum vaccine (51). The chemical composition of the bacterial polysaccharides, as well as their degradation by phage enzymes, has been reported for a number of *Klebsiella* and *Escherichia coli* strains (39). The physical structure of the branched polysaccharide of *E. coli* and its molecular packing has

only recently been described (42a).

In this report we describe: (i) the capsule morphology of *E. coli* strain Bi 161/42 [O9:K29(A):H$^-$] as seen in freeze-etchings, in ultrathin sections, and in air-dried preparations; (ii) the effect of increasing antibody concentrations on the capsular structure; (iii) the localization of sites of synthesis and "export" of the capsular polysaccharide in a temperature-sensitive mutant; and (iv) the filamentous substructure of the isolated polysaccharide after spreading on air-water interfaces.

## MATERIALS AND METHODS

**Cells.** We used the capsulated strain *E. coli* Bi 161/42, serotype O9:K29(A):H$^-$, originally isolated from a patient suffering from peritonitis (30). For detection of the O9$^-$ antigen, and for adsorption of the rabbit K29 immune serum, strain Bi 316/42 [O9:K9(L):H12] was employed; both strains were described by Kaufmann (31) and given to us by S. Stirm, Max Planck Institute for Immunbiology, Freiburg. Spontaneous, acapsular mutants of the capsulated strain were isolated from the agar culture plates and tested for the presence or absence of K29 antigen, for O9-agglutination, and for phage specificity. Two of these mutants lacking capsular antigen were used as "K$^-$" controls. Cultures were maintained at 37°C on nutrient agar; liquid cultures were started from single colonies after testing their K- and O-agglutinability on slides. Except for the temperature-sensitive mutants, which were grown at temperatures of either 46, 42, or 25°C, the liquid cultures of the wild type were grown at 37°C, either in shaking culture flasks or in aerated (bubbling) culture tubes, and kept in the range of $2 \times 10^8$ cells/ml.

**Media.** The nutrient medium consisted of 0.5% yeast extract, 1% tryptone (both Difco), 0.5% NaCl, and 0.1% glucose. The pH was adjusted to 7.0 by addition of 1 N NaOH.

**Bacteriophages.** The host cell for phage no. 29 is the capsulated *E. coli* Bi 161/42 containing the antigen K29. The phage does not adsorb to mutant strains lacking K29 antigen, as measured by agglutinability with anti-K29 serum. Another phage (abbreviated here as "capsule minus") has been used to test for cells lacking (fully developed) capsules, since it does not lyse, or attach to, bacteria of capsulated strain Bi 161/42, whereas it lyses all acapsular mutants tested. Both phages were provided by S. Stirm, Freiburg. (See also reference 60 for further characterization of the phages.)

**Isolation of temperature-sensitive mutants.** Mutants were selected that failed to produce capsular antigen at elevated temperatures (42 to 46°C). Liquid cultures of K29$^+$ cells were incubated for 24 h at 37°C with each culture in the presence of a different concentration of the mutagen ICR 191, a bisnitrogen (14). Mutagen concentrations of less than 40 $\mu$g/ml allowed cell growth, as indicated by increasing turbidity of the culture medium. Colonies obtained from such cultures were diluted ~$10^2$ times, spread on agar plates, replicated, and grown for 12 h at either 25 or 43°C. After this first plating, all colonies retained capsular antigenicity at 43°C. After a total of four replica platings, 7 of 33 colonies showed strong O-antigenicity at high temperature. These were tested for phage sensitivity with both the capsule-specific phage 29 and the capsule-minus phage that infects cells lacking a capsule. This was accomplished by growing cells for 4 h on nutrient agar at 43°C, then pouring prewarmed phage suspensions over the plates, and incubating for 12 h at 43°C (Table 1). Less than 5% of the colonies were killed by the capsule-specific phage, whereas only 0.2 to 2.5% of the colonies survived when incubated with the capsule-minus phage at that temperature. In parallel experiments, cells from single colonies of the seven strains were plated in a spiral pattern on rotating, prewarmed plates in dilutions high enough to permit counting of single colonies. After 4-h growth at 46°C, one-half of each plate was sprayed with a high-titer suspension of K29-specific phage. After another 12 h of incubation at 46°C, only those colonies were kept that produced 95% and more survivors. At lower temperature, these cells showed production of capsular antigen and phage 29 receptor. Six mutant strains with the desired temperature-sensitive character were further tested for their stability to maintain the capsular phenotype at lower temperature. After growth on agar plates for 14 h at 25°C in the presence of K29-specific phages, only 1 to 2.5% formed colonies compared to the number of colonies growing at 43°C. Cells to be used for temperature shift-down experiments were always taken from single colonies, plated, and grown overnight at 46°C; portions of such selected colonies were suspended, killed in broth by heating to 70°C for 30 min or by exposure to 2% formaldehyde, and subsequently tested for agglutinability with anti-K29 sera and O-specific sera.

Table 1 also shows that, of the mutants (designated f$^+$), all produced at permissive temperatures an obvious slimelike, fibrous material with capsule 29 antigenicity. This material was isolated and purified by methods identical to those used for the isolation of the wild-type K29 antigen.

**Isolation of the acidic capsular polysaccharides (APS).** In general, the procedures of Westphal et al. (64) were followed. These consist of the following steps: (i) phenol-water extraction. APS fractionates together with lipopolysaccharides (LPS) and nucleic acids into the aqueous phase; (ii) centrifugation at 100,000 $\times$ *g* to pellet LPS and associated nucleic acids; (iii) differential Cetavlon (cetyltrimethyl ammonium bromide) precipitation (54, 48) of nucleic acid and APS; (iv) dissolution of the APS in water and 3 times reprecipitation in alcohol; and (v) freeze-drying of the APS. In a number of preparations, ribonuclease treatment (26) in the beginning of step (iv) was included.

**Alkali treatment.** One milligram of APS was dissolved in 1 ml of 0.25 N NaOH, then heated to 56°C in a water bath for 1, 2, 4, 6, or 8 h, subsequently cooled to 4°C, neutralized with 1 N HCl, and dialyzed against distilled water.

**Preparation and purification of rabbit immunoglobulin G (IgG).** Suspensions (0.3 to 0.5 ml) con-

TABLE 1. *Mutant strains with temperature-sensitive production of capsular K29 antigen: survival in presence of K⁻ phage and agglutinability with anti-K29 serum and anti-O-serum*

| Mutant strain no.[a] | Colonies growing at 43°C | | Survival of colonies (%) | K29-specific agglutination after growth | | Slime production at 25°C | O-specific agglutination after growth | | |
|---|---|---|---|---|---|---|---|---|---|
| | O-specific phage absent from plate | O-specific phage present on plate | | 43°C | 46°C | | 25°C | 43°C | 46°C |
| 13 | 590 | 8 | 1.3 | ±[b] | −[c] | f+[d] | − | +[e] | + |
| 14 | 560 | 1 | 0.2 | ±[b] | NT[f] | − | − | + | − |
| 22 | 750 | 9 | 1 | + | − | f+ | − | + (weak)[b] quickly disappearing after shift down | − |
| 25 | 60 | 0 | NT | + | − | NT | − | + | − |
| 27 | 170 | 4 | 2 | + | NT | f+ | − | + | − |
| 33 | 250 | 6 | 2.4 | + | NT | f+ | − | + (weak)[b] | − |
| 41 | | | | ± | NT | f+ | − | + | − |

[a] In a few earlier publications (for example, reference 67), the prefix M was used to designate the mutants; this was later abandoned to avoid confusion with strains containing colanic acid.

[b] Agglutination delayed and visible only after >5 min, with the dark field microscope at ×15 magnification. (Cells were killed by boiling for 2 min.)

[c] −, Not agglutinating.

[d] f+, At permissive temperature colonies produce slimelike material.

[e] +, Agglutinating.

[f] NT, Not tested.

taining $2 \times 10^8$ cells/ml of either *E. coli* Bi 161/42 or Bi 316/42, boiled for 1.5 h, were injected into the ear veins of white New Zealand rabbits at intervals of 4 to 7 days. A week after injection five or six, blood was withdrawn by heart puncture, incubated at 37°C for 1 to 2 h, stored at 4°C for 15 h, and the serum withdrawn. The K-agglutination titer (against heat-killed K29 cells) was usually around 1:640; for O-antigen (using K⁻ mutant cells) it was 1:1280. The K29 antisera were repeatedly adsorbed with Bi 316/42 cells, until the O-antigenic titer was <4, whereas the K29 agglutination titer remained around 1:320, as determined by slide and tube agglutination. IgG fractions were obtained by a combination of sodium-sulfate precipitation (24) and column chromatography with QAE Sephadex A-50 (Pharmacia, Uppsala, Sweden) (F. Baum, Ph.D. thesis, University of Freiburg i. Br., Germany, 1972.): the globulin was precipitated once from serum by sodium sulfate, then dissolved in 0.9% NaCl, and dialyzed at 4°C overnight against diluted (1:2) ethylenediamineacetate buffer (EDA buffer) consisting of 2.88 g of ethylene diamine (distilled) and 73 ml of 1 M acetic acid, pH adjusted to 7.0. The QAE Sephadex column (42 by 2.5 cm) was adjusted with the same buffer. The globulin fraction, containing 40 to 60 mg of protein, was applied to the column in EDA buffer, and eluted by EDA buffer containing 0.1 M NaCl. The flow rate was kept at 5 ml/h. The agglutinating activity eluted in the first ultraviolet-absorbing peak and corresponded to the IgG fraction of the serum as shown by immune electrophoresis. The protein concentration was between 10 and 20 mg/ml, as determined by absorption at 280 nm with either lysozyme or bovine serum albumin as standard. The eluted IgG was concentrated by vacuum dialysis against 0.1 M phosphate buffer, pH 7.2, containing 0.9 g of NaCl per 100 ml.

**Affinity chromatography of anti-capsule IgG.** The conditions for the dissociation of the immune precipitate of anti-K29 IgG and K29 polysaccharide were established as follows. After a 1-h incubation at 37°C of a mixture of 0.2% solution of K29 antigen with anti-K29 IgG (10 mg/ml), the precipitate was washed 3 times in 0.9% NaCl. Four portions were stirred at 22°C into glycine buffer of pH 2.2, 2.6, 3.0, and 3.3. At pH 2.2, the immune precipitate dissolved immediately; at pH 3.3, about 1 h was needed, whereas at the pH of 2.6 and 3.0 the time for dissolving the precipitate was intermediate. Dialysis of these solutions against 0.1 M phosphate buffer, pH 7.0, led quickly to reprecipitation. We eluted the IgG from the K29 polysaccharide in the pH range between 2.0 and 3.0. To prepare the K29 polysaccharide affinity column, 20 ml of AH Sepharose 4B gel (120 to 200 mol of $NH_2$ groups) washed in distilled $H_2O$ was poured into 60 mg of K29 polysaccharide (pretreated with 0.25 N KOH for 1 h; ~120 μmol of carboxyl groups) was dissolved in 20 ml of distilled $H_2O$ and stirred at 22°C for 1 h. The pH was adjusted to 4.9 with 0.01 N HCl. One gram of 1-ethyl(3-dimethylaminopropyl)carbodiimide hydrochloric acid (Bio-Rad Laboratories, Richmond, Calif.) dissolved in 3 ml of distilled water was slowly added to the polysaccharide while the pH was held at 4.9 ± 0.1 by addition of 0.01 N HCl for 3 to 4 h. After stirring for an additional 16 h, the material was washed into a column with 1 M NaCl. The first 80 ml

of the effluent showed a positive sugar test with phenol/sulfuric acid (16). Subsequently, 150 ml of each of the following solutions was applied in sequence: 0.05 M barbital buffer, pH 8.5, plus 1 M NaCl; 0.05 M glycine/hydrochloride, pH 2.2, plus 1 M NaCl; and 0.05 M glycine/hydrochloride, pH 4.3, plus 1 M NaCl. The column was then equilibrated with 200 ml of 0.1 M phosphate buffer, pH 7.5, and 30 ml of anti-K29 IgG (5 to 10 mg/ml) was added in drops. The contents of the column were removed, stirred for 3 h at room temperature, then placed back in the column and washed with 0.1 M phosphate buffer until the eluate no longer caused any agglutination of K-specific bacteria. The column was further washed with 0.05 M barbital buffer, pH 8.5, until the ultraviolet absorption had dropped below 0.005. Finally the gel was treated with 30 ml of 0.05 M glycine buffer, pH 2.2, at 20°C and the flow stopped for 0.5 h, after which the outflowing protein, showing a pH of 2.8 to 3.0, was dialyzed against barbital buffer, pH 8.5; this elution was repeated once. The eluates were subsequently concentrated by vacuum dialysis in 0.1 M phosphate buffer of pH 7.0. IgG concentrations varying between 8 and 30 mg of protein per ml were used for ferritin conjugation and electron microscopic procedures. Ouchterlony immunodiffusion (49) was carried out at 21°C in 1% Agarose in 0.1 M barbital buffer, pH 8.2, with anti-capsule IgG and the extracted polysaccharides of the parent strain as well as of the mutants M41 and M13.

**Ferritin coupling.** Ferritin crystallized two times (Polysciences, Inc.) was recrystallized four times in $CdSO_4$ (24) and was conjugated with the purified IgG with xylelene/*meta*-diisocyanate (XMDI), again by the method of Hsu and Breese (24). For many of our experiments the XMDI was purchased from Polysciences. However, we also obtained XMDI prepared under National Institute of Health grants by K. C. Hsu, Columbia University, New York. The latter material appeared superior to the commercially available compound. Coupling with glutaraldehyde (33, 44) did not lead to comparable concentrations of active product.

**Light microscopy.** Cells from liquid cultures were mixed on the microscope slide with India ink (Pelikan) in a volume ratio of two parts cells ($2 \times 10^8$/ml) to one part ink. Oil immersion objective (numerical apperture, 1.25) and, frequently, additional phase-contrast optics were employed. Micrographs were taken with either a Zeiss photomicroscope or a Zeiss research microscope, the latter equipped with a Leica MI on a Leitz Orthophot stand. Since the cells were tumbling due to Brownian motion, an electronic flash (Zeiss) served as light source for exposures on Kodak Plus X Pan film.

**Electron microscopy.** (i) Ultrathin sectioning cultures from single colonies of the wild-type strain Bi 161/42 and of the revertants were grown in aerated nutrient broth at 37°C until cell densities of 1 to $3 \times 10^8$/ml were reached. Colonies of temperature-sensitive mutants were grown overnight on nutrient agar at 46°C, quickly transferred to a tube with 46°C nutrient broth immersed in a precision water bath, and aerated with prewarmed air of 46°C until densities of $10^8$ cells/ml were obtained. For initiation of capsule production, these cells were rapidly transferred to media of lower temperature, usually 25°C, and grown for various lengths of time. After subsequent reactions either with antisera, ferritin-conjugated antibody, or with phages (see below), the cells were fixed at room temperature in 2% formaldehyde, made from paraformaldehyde, and added to nutrient broth at pH 7.0. In some experiments, the nutrient broth contained 20% sucrose (wt/vol) to induce plasmolysis (13). During fixation, the pH was kept around 6.5 to 7.0 by occasional additions of small amounts of 0.01 N NaOH. After 1 h of fixation, the cells were sedimented at $4,000 \times g$ and suspended in 1% osmium tetroxide-nutrient broth (which also contained 20% sucrose whenever the cells had been exposed to sucrose in the prior step). One hour later, the cells were sedimented again and briefly washed in 1% $OsO_4$ dissolved in $H_2O$ (plus 10% sucrose for those cells that were previously plasmolyzed), then exposed at 20°C for 30 min to a mixture of 1% $OsO_4$ and half-saturated uranylacetate. The material was subsequently dehydrated and embedded in Mollenhauer medium (Epon Araldite) (42) or in Vestopal (both from Polysciences), incubated for polymerization at 55°C for 48 h, and sectioned with diamond knives in an LKB Ultrotome. The sections were stained with uranylacetate and lead-hydroxide (50). When ruthenium red (Electron Microscopy Laboratories and Polysciences) was used, it was dissolved in water, then filtered through membrane filters (Millipore) of 0.45-$\mu$m pore size and added in half-saturated concentrations to both fixation fluids, the aldehyde and the $OsO_4$. The solubility of these mixtures was tested before, since some batches of the available ruthenium red started to precipitate in the fixation mixtures. We found that after aldehyde treatment, $OsO_4$ fixation, and subsequent washing of the cells, the agglutinability by anti-K29 sera remained unimpaired; also the receptor activity for phage 29 was retained. If the cells, either unfixed, or fixed and washed, were to be reacted with antibody, rabbit anti-K29 IgG (of agglutination titers 1:320) was applied in concentrations of 2 to 4 mg/ml at 0°C for 30 min; the cells (which were agglutinated by the antibody) were sedimented twice at $2,000 \times g$ for 10 min, and suspended in 0.1 M phosphate buffer, pH 7; for the indirect ferritin-labeling method, the ferritin-conjugated anti-rabbit IgG was added at 0°C to cells that had been pretreated for 10 or 30 min with unlabeled rabbit anti-K globulin. Forty-five minutes later, the cells were sedimented at $2,000 \times g$, washed twice in phosphate buffer, and fixed for 30 min in $OsO_4$ or osmium tetroxide-uranylacetate, and finally embedded as described above.

(ii) For negative staining of whole-cell preparations, a drop containing the suspended cells was placed on a Formvar-coated electron microscope grid, the staining fluid was added, excess fluid was blotted off, and the preparation was dried in the vacuum of the electron microscope. When whole cells were to be antibody-treated on the grid, the Formvar-coated grid was first exposed for about 1 min to a 1% bovine albumin solution and washed, before cells and con-

jugated immune globulin were added. This procedure reduced the ferritin background of the support film considerably. For the virus adsorption studies, phage 29 was always freshly purified on CsCl gradients to avoid the possible interference from small-sized capsid fragments containing capsule-degrading enzymatic activity (57); the phage was used after dialysis against either nutrient broth or phosphate buffer. In parallel with the microscopic preparations, the phage adsorption kinetics were studied in test tube cultures so that we were able to estimate the number of adsorbed phages to be expected in ultrathin sections. Phage adsorption was determined by the decreased titer of the unadsorbed phages after dilution and ultrafiltration (4).

(iii) Freeze-etching was performed with either unfixed or fixed cells (see below) in a Balzer BA 360, at −100°C for 1 to 3 min. Platinum and carbon evaporation, and subsequent steps, were executed as in (3).

(iv) For the spreading of polysaccharide on air-water interfaces, we followed, in general, the methods of Kleinschmidt and Zahn (35) and Kleinschmidt (34) that these authors employed for nucleic acid molecules.

## RESULTS

**The morphology of the capsule.** The capsulated *E. coli* strain Bi 161/42 grows at 37°C in aerated medium with an average generation time of 25 min. The size of these cells was measured in the light microscope (phase contrast) to be 1.2 μm in width and 2.5 μm in length. The majority of the cells were plump rods, about 25% of them showing septation and late stages of separation. India ink preparations revealed a much increased diameter of the cells due to the conspicuous capsule that prohibits the ink particles from approaching the surface of the cell wall; thus, the cells retain a transparent halo, which adds to the cell contour about one-third to one-half of the cell's diameter. Combination of phase-contrast illumination with India ink revealed the contour of the capsule as well as that of the cell envelope and the protoplasmic contents (Fig. 1). None of the features of the capsule was observed in the strains lacking agglutination with K29 antiserum. The "slime"-producing temperature-sensitive (f) mutants showed a rather hazy, ill-defined zone of very uneven thickness around the cell.

The use of ferritin-conjugated anti-K29 globulins as well as the application of indirect ferritin label (unlabeled rabbit anti-K29 globulins followed by ferritin-conjugated anti-rabbit globulin) showed a capsule of considerable dimensions (Fig. 2), with a thickness varying between 400 and 600 nm. Also, the use of unconjugated anti-capsule IgG revealed the capsule, although with much less contrast than with the ferritin-labeled IgG. It is obvious, however,

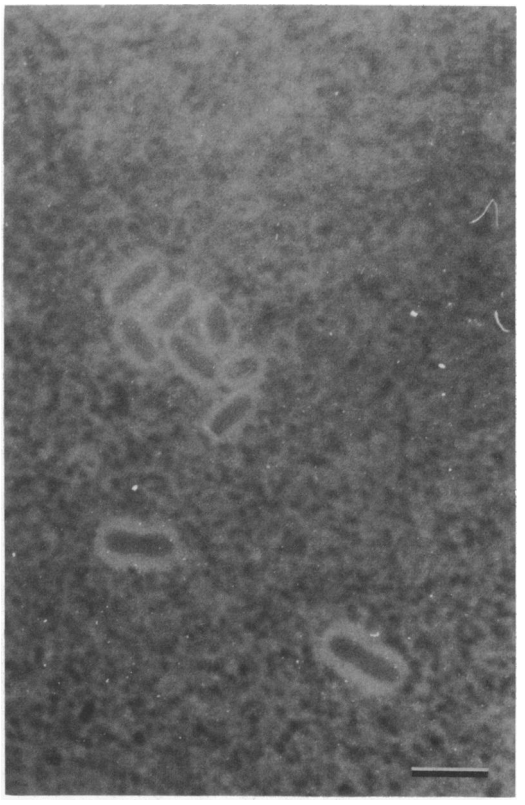

FIG. 1. *Light micrograph of E. coli Bi 161/42 suspended in liquid India ink; the contour of the cells shows a halo around the cells due to the exclusion of the ink particles by the capsular material. Phase contrast, ×1,800. The bar represents 2 μm.*

that in such air-dried whole-cell preparations, the capsule has been flattened by the surface tension of the water during the drying process. Treatment of the capsulated cells with either 4% phosphotungstic acid, silicotungstate, or 2% osmium tetroxide showed no conclusive evidence for the existence of an extended capsule, although after such negative staining the electron density appeared to have conspicuously increased in the area immediately surrounding the cell envelope (Fig. 3). Unstained preparations did not show any sign of capsular material. We attempted to preserve the capsule during dehydration and embedding for the purpose of ultrathin sectioning; however, such treatment resulted in the production of thick bundles of material with relatively high electron contrast located external to the cell's outer membrane (Fig. 4). Fixation in the presence of ruthenium red (40, 55) did not have any apparent capsule-stabilizing effect. Only occasionally a small number of cells was seen with a seem-

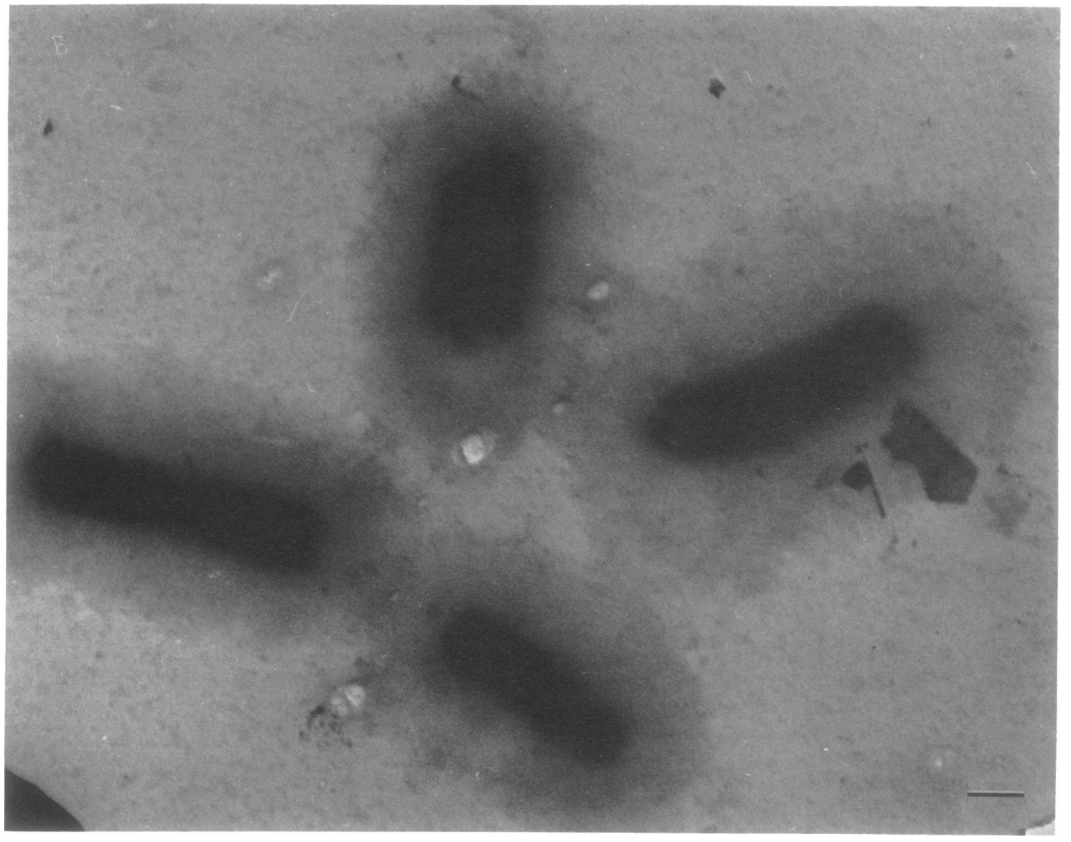

FIG. 2. *Capsulated E. coli after treatment with ferritin-conjugated IgG directed against antigen K29.*

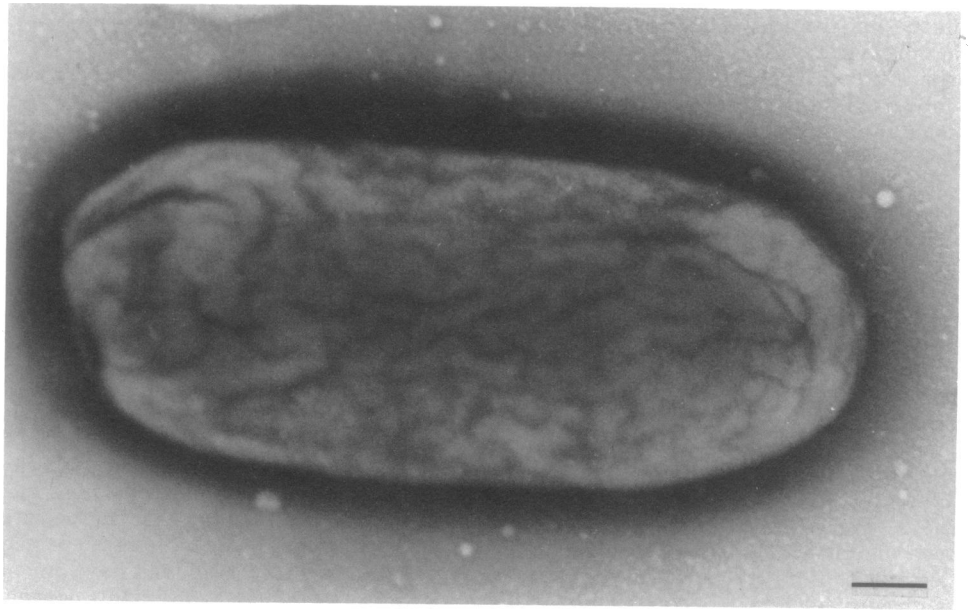

FIG. 3. *Electron micrograph of a capsulated E. coli after negative staining in 2% silicotungstate. The extended amorphous zone of high electron contrast around the bacterium is seen only in capsulated cells. The bar in this and the subsequent micrographs represents 250 nm.*

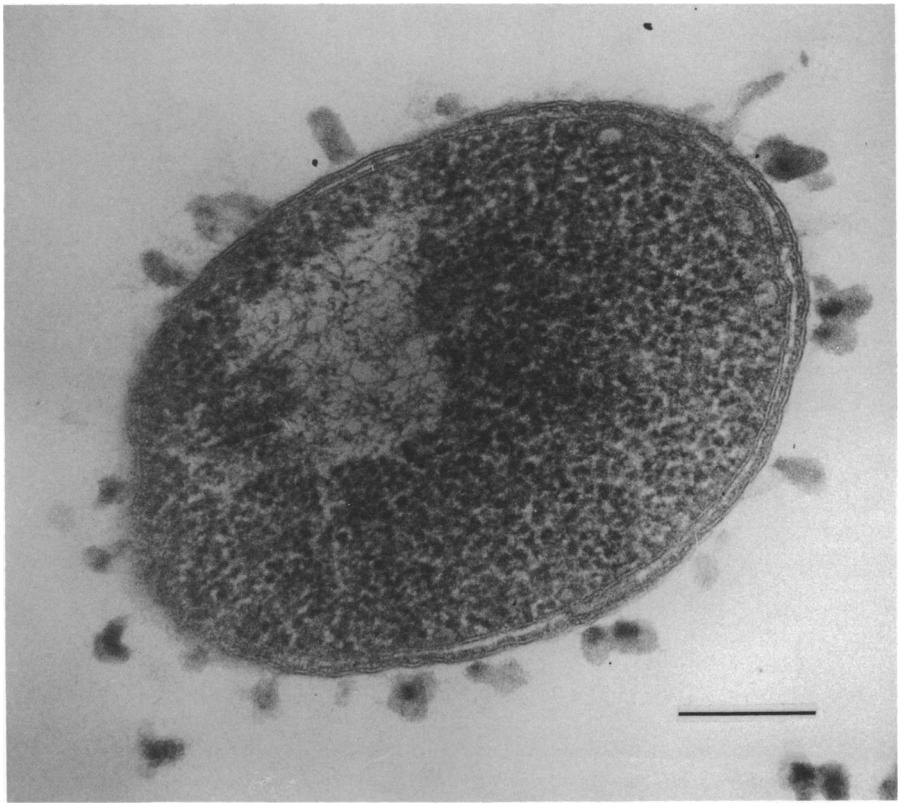

FIG. 4. *Typical aspects of shrinkage and clumping of the E. coli capsule as seen in ultrathin sections after fixation, dehydration, and polyester embedding.*

ingly delicate web in the area of the capsule measuring about 200 nm in thickness; this structure could represent the capsule in a relatively uncollapsed state (Fig. 5). To find out at which preparative step the collapse of the capsules occurred, we employed the freeze-etching method. We kept the step-by-step pretreatments identical to the procedures conventionally employed for fixation and different degrees of dehydration. We found that the capsule collapsed during the early steps of dehydration, after 10 min in 50% acetone (Fig. 6). Return of the specimen into water for 10 min (before subsequent freezing) did not reestablish the original amorphous shape of the capsule.

When fixed or unfixed cells were quickly frozen (without dehydration) and subsequently freeze-etched, a generally smooth capsular surface was seen, occasionally interrupted by stringy filamentous elements. There was no evidence for any organized fine structure such as filamentous subuntis. Cells just jutting over the receding ice surface often revealed numerous conical, spine-like projections protruding over the otherwise smooth, sometimes stringy capsule surface (Fig. 7). Uncapsulated revertants exhibited a surface typical for acapsular gram-negative bacteria (Fig. 8 [3, 4, 45]). It was unexpected that capsulated cells, after deep etching, failed to reveal a pronounced capsular cover comparable to the dimensions shown in the light microscope (India ink) preparations. We suspect that, as the ice sublimates, increasing portions of the capsule are insufficiently anchored and are lost into the vacuum during etching (at −100°C). Such a release of structures into the vacuum during freeze-drying has been postulated by Anderson (Proceedings of the International Conference on Electron Microscopy, London, p. 122–129). In both freeze-fractured (no etching) and briefly freeze-etched preparations of capsulated cells, an obvious delineation of the cross-fractured capsule against the surrounding ice was not detectable, probably because of the high water content of the capsule. However, a pronounced demarcation of the capsule occurred after treatment with sufficiently high concentrations of capsule-specific antibody (Fig. 9); then the capsule resembled "table mountains," in which the capsular coat measured between 100 to 300 nm in thickness. The capsule was always seen to cover the

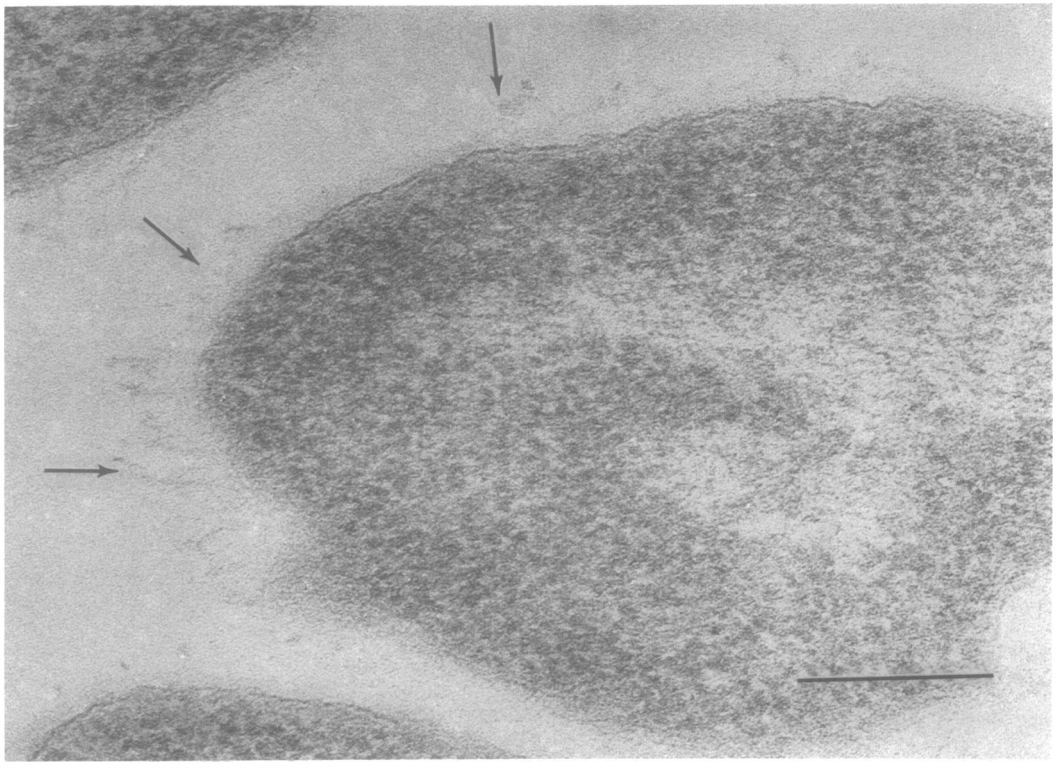

FIG. 5. *A small number of cells reveals a faintly contrasted zone of capsular material (arrows) around the sharp contour of the surface of the outer membrane.*

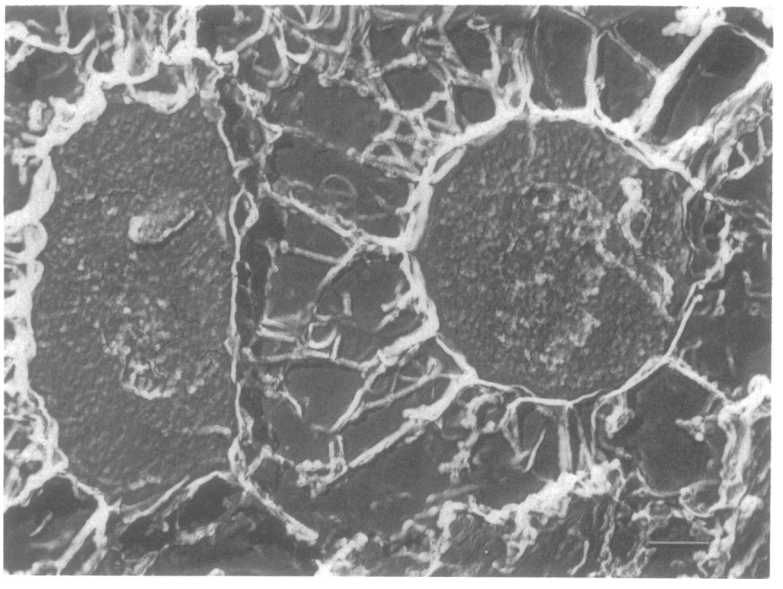

FIG. 6. *Freeze-etching of capsulated cells after 5 min of dehydration in 70% acetone and subsequent brief washing in nutrient medium. The capsular material has shrunken to filamentous structures that extend from one cell to the next one. Cf. Fig. 4.*

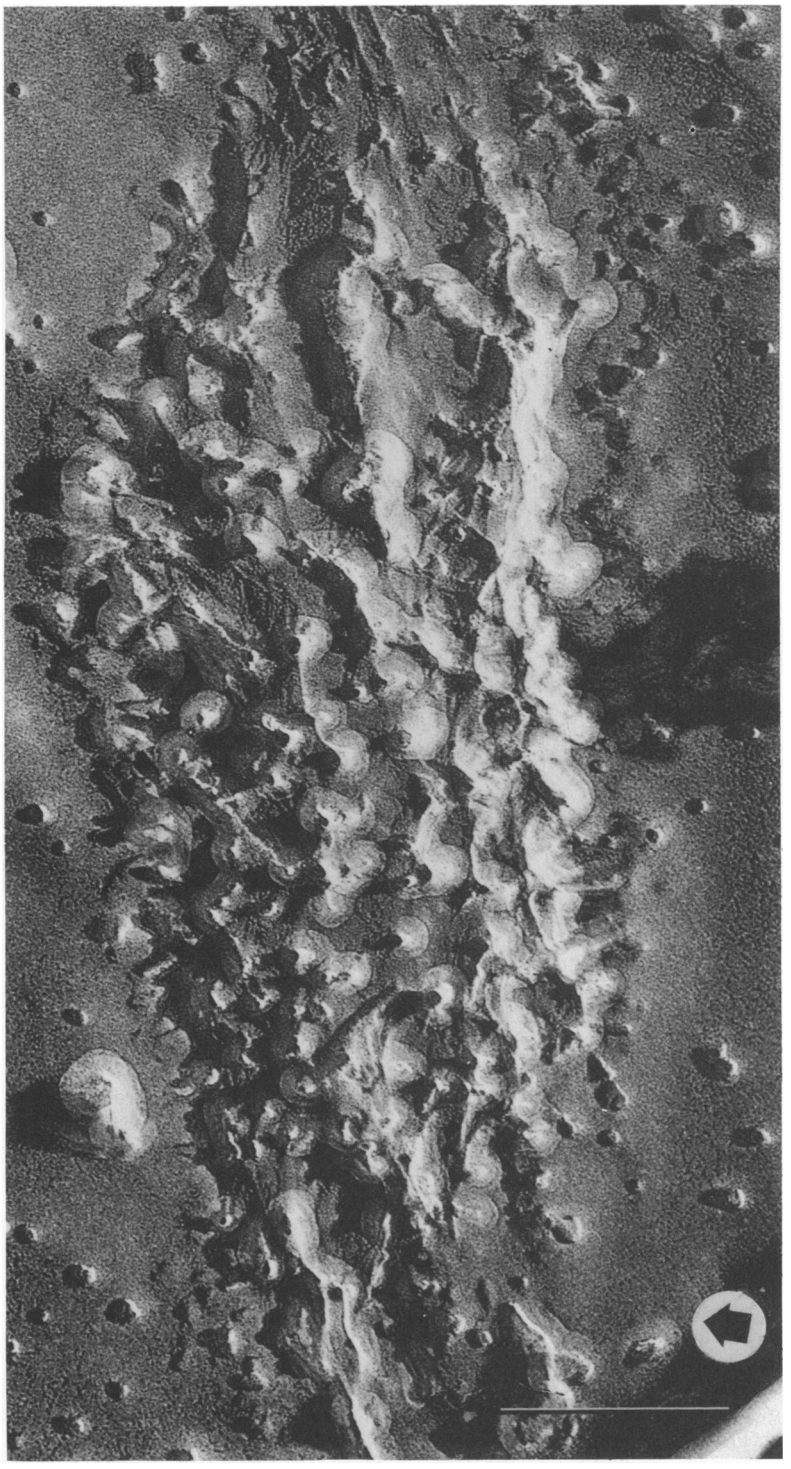

FIG. 7. *A capsulated cell after freeze-etching. While most of the cell is still buried in the ice, the capsular surface becomes visible as multiple spines protruding over the plateau of the surrounding frozen medium. These structures seem to become less obvious after longer etching times. Some filamentous elements can be seen at top and bottom of the micrograph. (The broad arrow on white background indicates the direction of shadowing in preparations for which platinum-carbon shadow casting was employed.)*

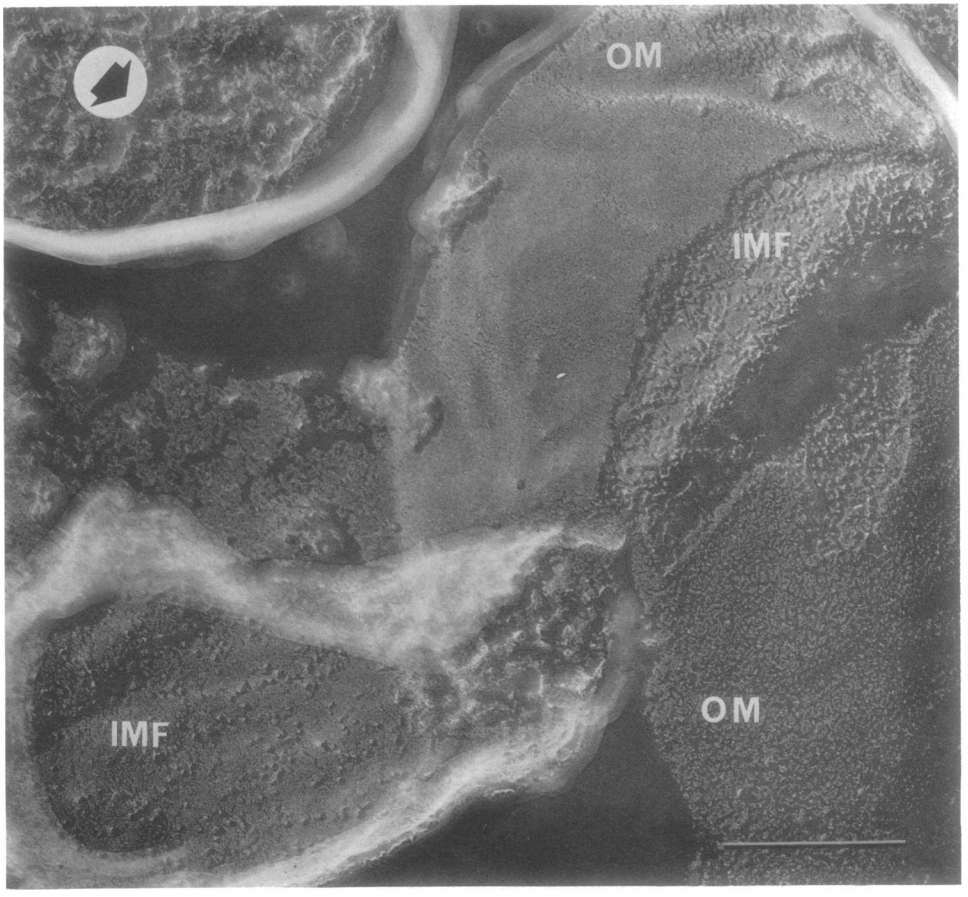


FIG. 8. *The surface of an acapsular revertant cell appears identical to the surface of other, noncapsulated gram-negative bacteria. Exposed are the outer membrane (OM) and the convex fracture plane of the protoplasmic membrane (inner membrane, IMF). At the left side of the figure, a membrane piece is cleaved off and turned over, exposing the concave fracture plane of the protoplasmic membrane (IMF). An area of low-shadowing angle has been selected to affirm the absence of fibrous material. (Broad arrow indicates direction of shadowing as in Fig. 7.)*

entire surface of the cell envelope. Thus, the total diameter of antibody-treated capsulated cells measured 1,500 to 1,800 nm. The concentration of the K-specific antibody had a significant influence on the dimension and shape of the resulting capsular structure: IgG (with an anti-capsule titer of $\geq$1:164) at concentrations of 0.01 mg of protein per ml had little or no effect on the apparent thickness of cross-fractured cell envelopes. At IgG concentrations of 0.1 mg of protein per ml, a significant layer of material around the contour of the cell envelope was observed (Fig. 10) with a tendency to form long, starlike projections, often connecting neighboring cells. At higher antibody concentrations, such as 0.3 to 0.5 mg/ml, the capsule assumed the rather solid-looking structure described above (see Fig. 9), which surrounds the envelope with a layer of relatively uniform thickness. To exclude the possibility that such a thickening might be caused by the nonspecific adsorption of proteins, we studied: first, capsulated K29 cells after exposure to (i) 0.5 mg of K29-specific IgG per ml and (ii) 0.5 mg of anti-rabbit IgG per ml, from goat, lacking K29 specificity; second, uncapsulated mutants exposed to (i) 0.5 mg of K29-specific IgG per ml and (ii) 0.5 mg of nonspecific anti-rabbit IgG per ml from goat.

After freeze-etching, a thickening of the areas around the cells was only found after interaction of the capsule with K-specific IgG. The controls ([ii] of the possibilities studied) showed no sign of thickening; in the case of capsulated K29 cells exposed to anti-rabbit IgG from goat (without K29 specificity), a ragged,

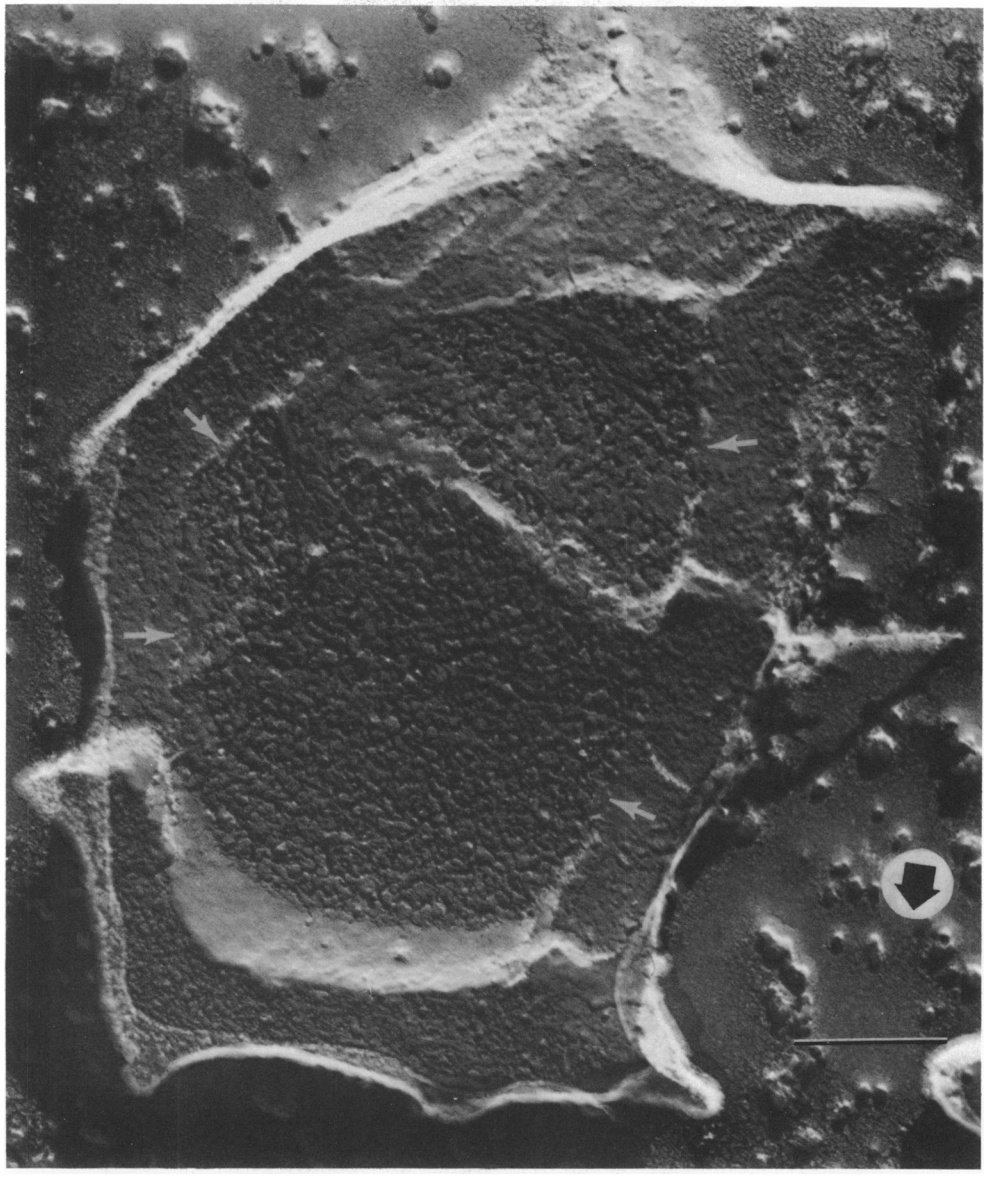

FIG. 9. *Addition of anti-capsule (K29) IgG at relatively high concentrations (0.5 mg/ml) reveals a thick homogeneous capsular "coat" in the freeze-etching replicas. The border between the protoplasmic contents and the capsule (arrows) is clearly delineated by the cleavage plane(s) within the cell envelope. (Broad arrow indicates direction of shadowing as in Fig. 7 and 8.)*

sometimes stringy cell surface indistinguishable from that described above for the surface of untreated capsulated cells was seen (see Fig. 7). These results show that the thick layer, visible after anti-capsule IgG, is the product of a specific reaction between capsular antigen and antibody. Bacteria, treated with 0.3 mg of K29-specific antibody per ml prior to fixation, dehydration, and embedding, reveal also in ultrathin sections a conspicuous capsule as a contrasting, relatively dense coat measuring 150 nm to 350 nm in thickness (Fig. 11). Due to the presence of antibody, the cells were mostly agglutinated. A fine structure of the capsule was occasionally suggested by fibers, apparently being radially oriented and producing a texture as shown in Fig. 12. In agreement with the freeze-etching data, the capsule showed a rela-

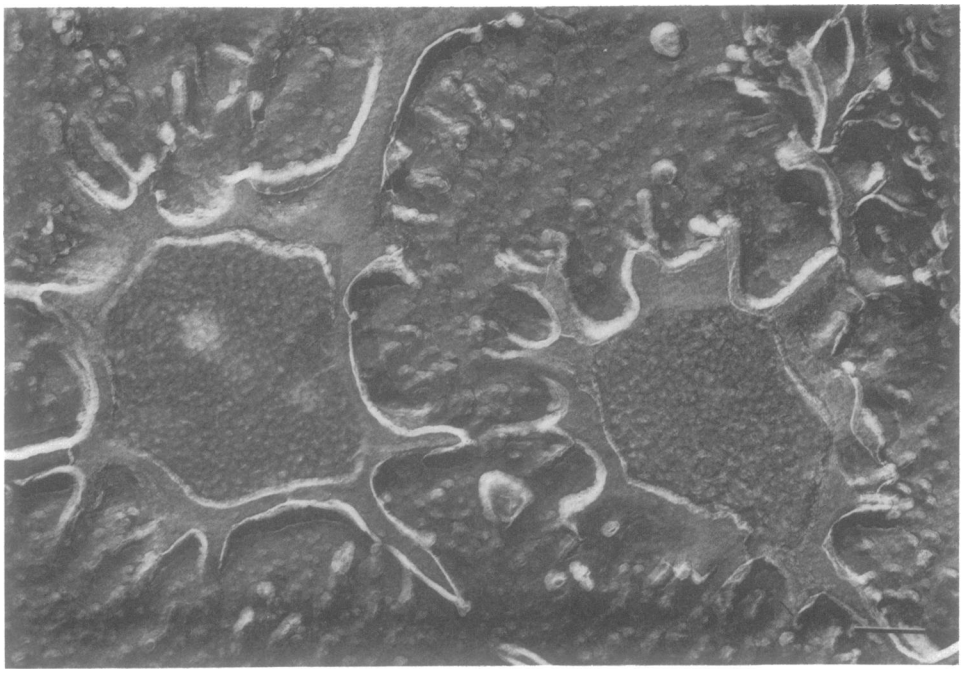

FIG. 10. *Freeze-etching replica of capsulated cells after treatment with anti-capsule IgG (0.1 mg/ml), which is a lower concentration than that employed in the preparations shown in Fig. 9. Note the reduced thickness of the capsule and the spiny extensions.*

tively smooth surface contour. Ultrathin sections of the acapsular mutants revealed the typical surface features of noncapsulated gram-negative bacteria (Fig. 13).

**Capsular mutants.** Mutants 13, 22, 27, and 41 (see Table 1) grown at permissive temperatures (below 46°C) agglutinated with K29 antiserum; these cells produced a stringy material with K29 antigenicity, generating a surface entirely different from that of the wild-type capsule: India ink failed to delineate a well-defined contour of the cells. Treatment of the unfixed whole cells with ferritin-conjugated anti-K29 IgG revealed long filaments emerging from the cell surface (Fig. 14). The diameter of the filaments varied, but always decreased with the distance from the cell; their length was difficult to establish; some filaments measured 10 to 15 $\mu$m in length, yet others seemed to stretch over distances of 2 to 3 neighboring fields of the electron microscope (400 mesh) grid, suggesting a length of over 150 $\mu$m for these bundles. In addition, the filaments showed a tendency to associate with the filamentous material from neighboring cells, so that the total length of filaments originating from individual cells could generally not be determined; in cultures of higher cell densities, one has to assume that a loose three-dimensional meshwork of polysaccharide filaments exists between the cells, involving also free polysaccharide strands. Free polysaccharide could be isolated from the cell-free supernatants of these cultures, and caused a considerable increase in the viscosity of the culture media.

When the temperature-sensitive mutant 13 was grown at the nonpermissive temperature (46°C), its surface structure was indistinguishable from that of an uncapsulated cell, and ferritin-conjugated anti-K29 IgG did not seem to bind to the cell (Fig. 15). However, 10 to 15 min after shift down to 25°C, ferritin-conjugated anti-K29 IgG started to bind to the cell surface (Fig. 16); agglutination by anti-K29 IgG became detectable (by tube agglutination) after 10 to 20 min (Table 2). Table 3 shows that the capability of the cells to adsorb the K-specific phage 29 became measurable around 15 min after shift down. Adsorbed phage 29 particles were demonstrable (in ultrathin sections) about 20 min after temperature shift down (M. E. Bayer and H. Thurow, manuscript in preparation). Two hours after shift down were required to reveal in the light microscope (using India ink stain) the first signs of an ill-defined halo around the mutant cells.

**Antigen "production" sites.** To determine number and location of the antigen export sites,

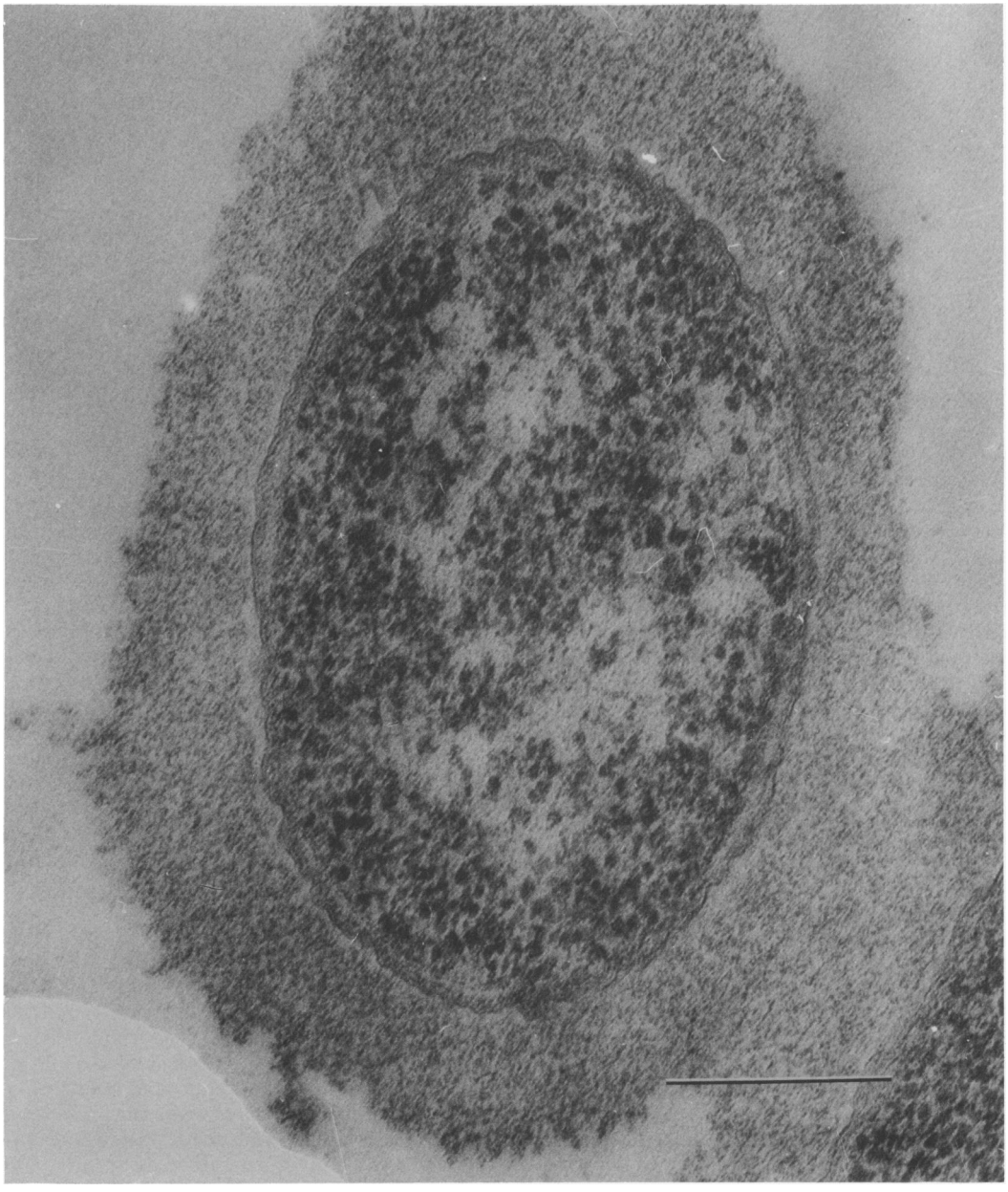

FIG. 11. *Ultrathin section through capsulated E. coli treated with high concentration (0.5 mg/ml) of anti-capsule (K29) IgG before dehydration and embedding. The capsule appears to be rather uniform in thickness. Cf. Fig. 4.*

we studied ultrathin sections of mutant M13 exposed to conjugated anti-capsule IgG after temperature shift down and subsequent growth for 15 to 20 min at 25°C. We found between 10 to 40 polysaccharide export sites per productive cell (see Fig. 16 and 18). In later times after shift down, either more export sites had appeared, or more capsular antigen was produced; unfortunately, it became increasingly difficut to decide whether the material had been spreading laterally or had readsorbed and engulfed the cells. Also, it seemed that polysaccharide had been released into the intercellular space (see Fig. 18). The early export sites of the

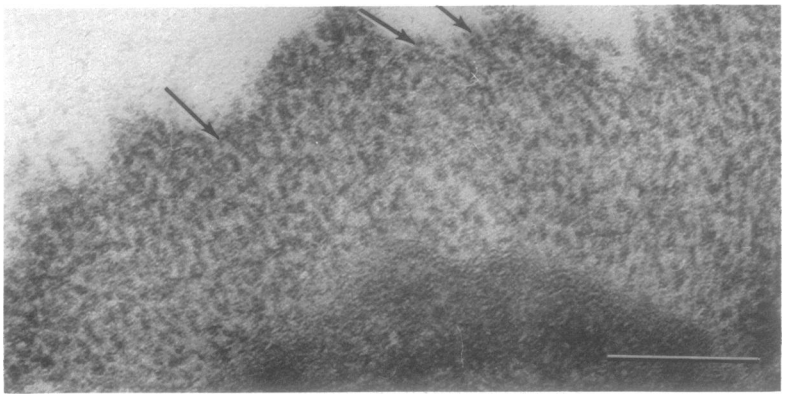

FIG. 12. *In this ultrathin section the capsule appears to reveal a fibrous composition (arrows).*

polysaccharide were revealed as ferritin-labeled filaments, or delicate strands, protruding from the outer membrane into the medium. Very frequently the emerging filament was seen at an area at which cell wall and protoplasmic membrane adhered to one another (Fig. 17); these adhesion sites become visible only after slight plasmolysis (1) and have previously been shown to be involved in a variety of envelope functions (2). An additional conformation of the newly synthesized polysaccharide was the cluster (see Fig. 16 and 18); the clusters appeared to represent coiled filaments. These two conformational aspects, as well as the limited number of capsule-producing areas per cell, were also observed in freeze-etched preparations; within 15 min after temperature shift down, ferritin-conjugated IgG molecules delineated filamentous structures (arrows, Fig. 19) as well as small clusters of antigen (Fig. 19). Acapsular cells did not show such particle arrangement. It was also obvious from both the sections and the freeze-etched replicas that the cells did not start making capsular substances in synchrony; instead, a considerable variation in the occurrence and in the amount of ferritin label among the cell population was found for early times (10 to 15 min) after shift down. At later times (45 to 60 min), almost all of the cells showed at least some ferritin label at their surface.

**Filamentous elements of the isolated capsule polysaccharide.** To convert a "nonuniform" superstructure of isolated polysaccharides to greater uniformity of size (9, 25, 27, 47), the purified capsular polysaccharide of the wild-type cells was treated with 0.25 N NaOH for different lengths of time. In immunodiffusions against anti-K29 IgG, the polysaccharides of mutant 13 and 41 show lines of identity with the wild-type polysaccharide as well as with the alkali-treated (4 h) material (Fig. 20).

The effect of alkali treatment on the morphology of the isolated K29 polysaccharide was seen after spreading the polysaccharide on an ammonium carbonate buffer, pH 7.0, in analogy to the methods used for length measurements of nucleic acid molecules (34, 35). Although spreading was mostly done in the presence of cytochrome *c*, the protein was not obligatory for such spreading to occur; however, its presence increased the yield of recognizable molecules in the preparation. We found in the untreated K29 polysaccharide preparations, long, relatively thick bundles with finer strands branching off, in a few instances showing free ends (Fig. 21a). Other morphological aspects were large, twisted circular arrangements (Fig. 21b). After 2 h of alkali treatment, and even more so after 4 h of treatment, most of the large bundles had disappeared and very fine filaments became visible (Fig. 22). These filaments were often seen to have branched off from the still undissociated larger bundles. A "smallest class" of isolated filaments was frequently observed. They measured from 3 to 6.6 nm in width and around 250 to 350 nm in length (Fig. 22). A characteristic feature was the presence of a "knoblike" element of about 10 nm in diameter at one end of the fiber (Fig. 22). The other end of the fiber often seemed to taper off, or to case a lower shadow, making accurate length determinations difficult. Considerably shorter filaments, of 150 nm or less in length, were found only in relatively few instances. Alkali treatment for 6 h drastically decreased the number of the thin filaments as well as the visibility of the knoblike element. Very few larger bundles were observed. After 8 h of treatment, most of these structures were absent, and, very rarely, an isolated fiber-like structure was seen; some ill-defined, possibly

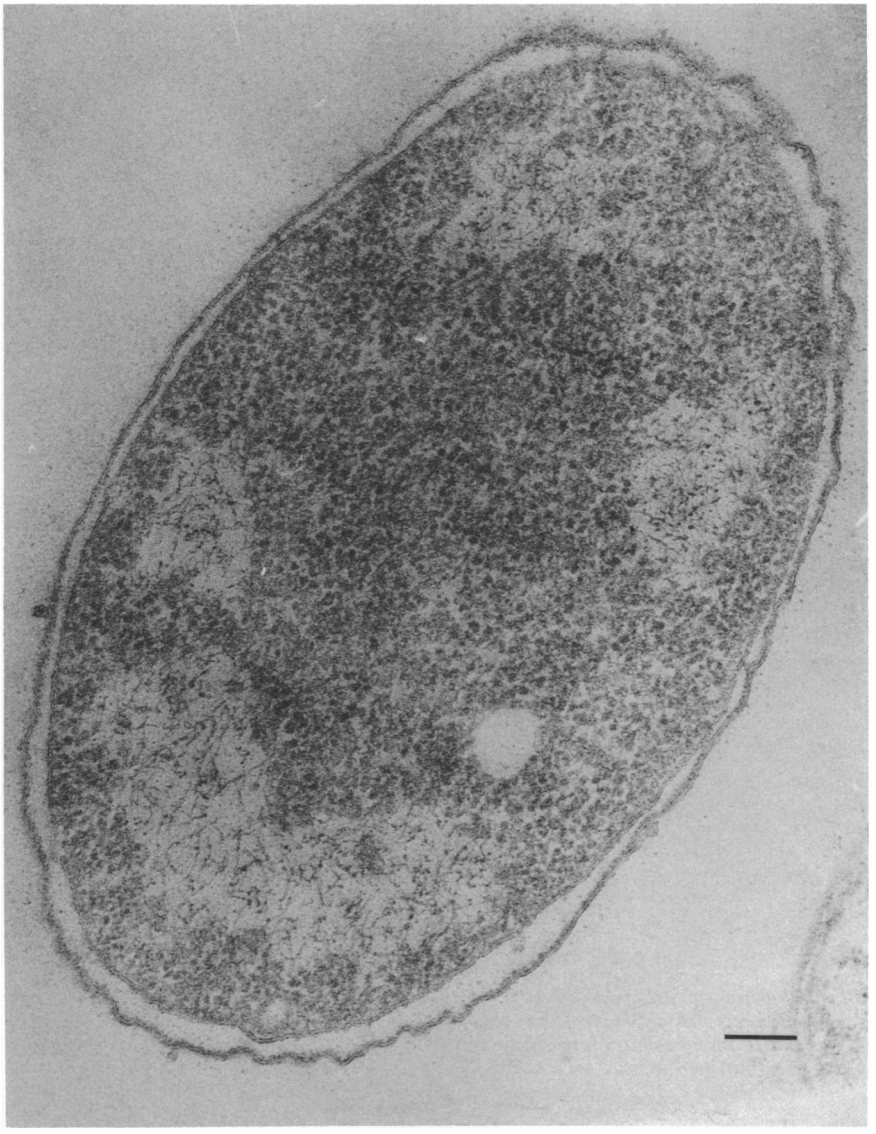

FIG. 13. *Ultrathin section of an acapsular revertant, pretreated identically to capsulated cells shown in Fig. 11 and 12. The cells are totally devoid of "capsular" reaction products.*

netlike clusters with very-low-shadow profiles were observed.

## DISCUSSION

We have demonstrated that the highly hydrated capsule of *E. coli* is a relatively uniform gel of 250 to 300-nm-average thickness lacking any pronounced fine structure. The capsule excludes larger particles such as carbon particles of India ink. This reaction causes, in the light microscopic preparation, a halo of several hundred nanometers in thickness to appear. For observations in the electron microscope, the capsule had to be stabilized with anti-capsule globulin. Under these conditions, the capsule formed a layer of about 300-nm thickness, without any striking fine structure, except for the occasional occurrence of fibrous elements. On a dry weight basis, the capsule of *E. coli* Bi 161/42 amounts to 7.5% of the total weight of the cell, as measured by the phenol-cetavlon extraction procedure (9); thus, the *E. coli* capsule is as rich in water content as the capsule of many

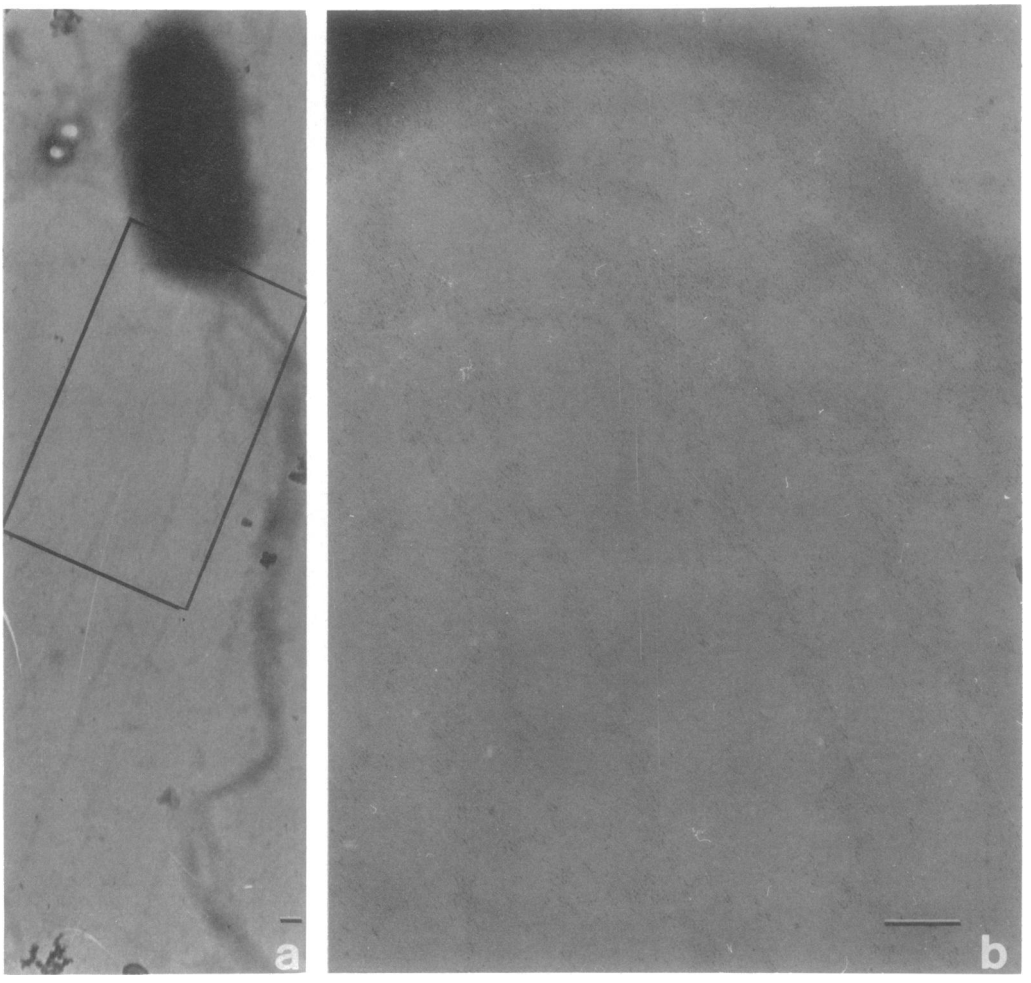


FIG. 14. *Temperature-sensitive mutant 41 after shift down from 42°C and growth for 2 h at 25°C. The electron microscopic preparation is identical to that of the parent cells seen in Fig. 3. The cell in (a) shows long filaments stained with ferritin-conjugated anti-capsule IgG. Insert (b) represents a higher magnification of the rectangular area outlined in (a).*

other bacteria (65, 66). The task for the structural preservation of such an organelle during dehydration is magnified by the propensity of the polysaccharides not to cross-link or stabilize during common fixation procedures; we observed that the "fixed" capsule still reacts with its antibody and also adsorbs capsule-specific phages.

A bacterial capsule was demonstrated by 1943; employing the electron microscope in the study of air-dried preparations of antibody-treated pneumococcus (43), a rather thick, ill-defined zone of low contrast was seen that surrounded the much denser contour of the cell. In contrast to this, some capsules have been reported to reveal considerable structural detail, such as the spindle-shaped striated elements of the capsule of *E. coli* Lisbonne strain (36), the fibrillar elements of the cellulose-containing capsule of *Acetobacter xylinum* (11), as well as the complex capsule of *Mycobacterium lepraemurium*, with its fibrillar structure surrounding the bacterium, possibly serving as barrier to the action of enzymes of the infected cell (15). Fibrillar, intercellular structures were also described for the extracellular polymers of a variety of anerobic bacteria (7). To stabilize and possibly stain (19) the acidic polysaccharides we used ruthenium red, which had been employed to demonstrate the polysaccharides of higher cells (40) as well as those of *Streptococcus pneumonia*, *Klebsiella* species, and other microorga-

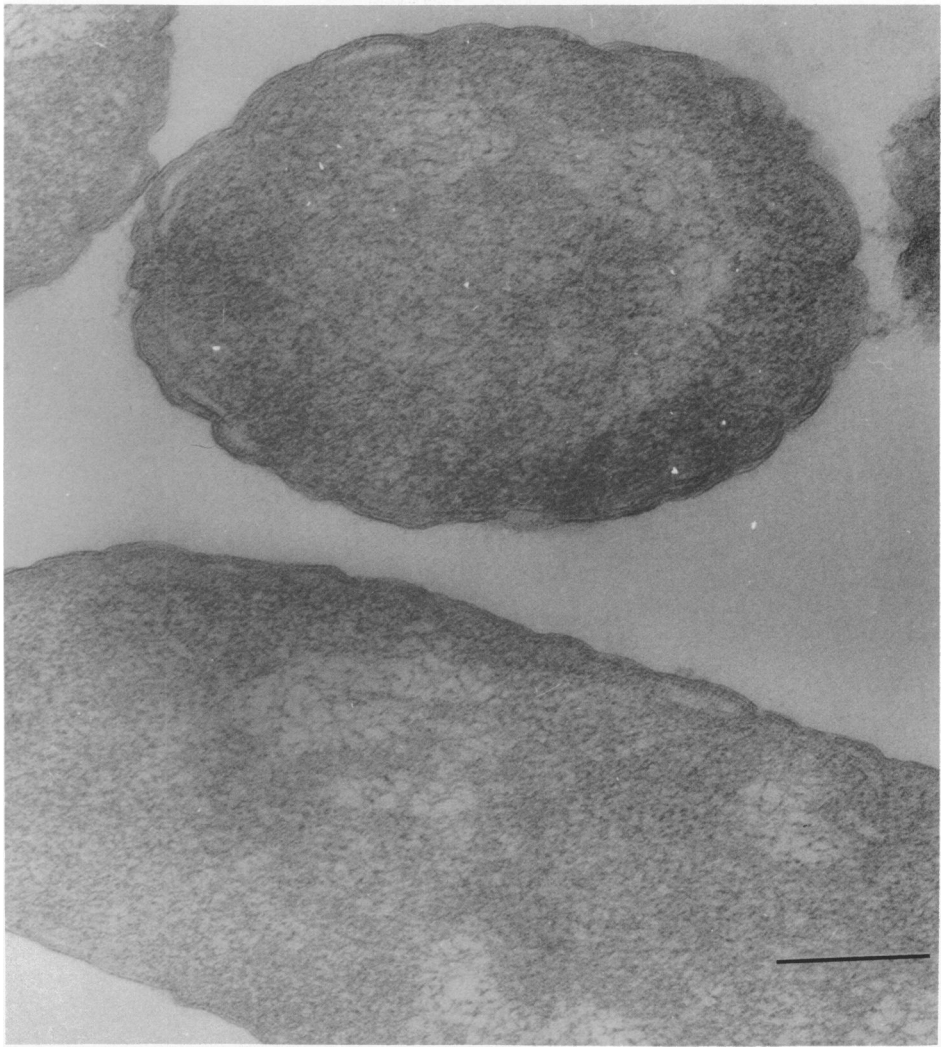

FIG. 15. *Ultrathin section of mutant 13, grown at 42°C, rapidly cooled to 4°C, and treated at 4°C with ferritin-conjugated anti-capsule (K29) IgG before fixation and embedding. There is almost no ferritin "background" visible.*

nisms; in these cells, fibrous and netlike capsules were found (7, 8, 55, 56). We had previously employed this reagent with two capsulated strains of *E. coli*, which contained K-antigens 26 and 29, and found in both strains in a few ultrathin sections a faint, veillike structure surrounding a small number of the cells (M. E. Bayer, Bacteriol. Proc., p. 43, G119, 1971), whereas in most of the cells of *E. coli* Bi 161/42 the capsular substance had been deformed to thick bundles of high electron contrast. This aspect did not resemble that of the nondehydrated cell seen in the light microscope. Clumping of the capsule was not observed after freeze-etching; while fixation with aldehydes and osmium tetroxide had no visible effect on the structure of the freeze-etched capsule, dehydration for only a few minutes in 50 to 70% alcohol or acetone caused the capsule to collapse into a number of relatively thick clusters or fibers. The fine "strands" that we observed in the freeze-etched, uncollapsed capsule might represent polysaccharide bundles associated with each other by forces that can be broken by treatment with NaOH, as seen in the isolated polysaccharide. That one finds an obvious capsule with the "spiny" surface on those cells that only barely protrude over the plateau

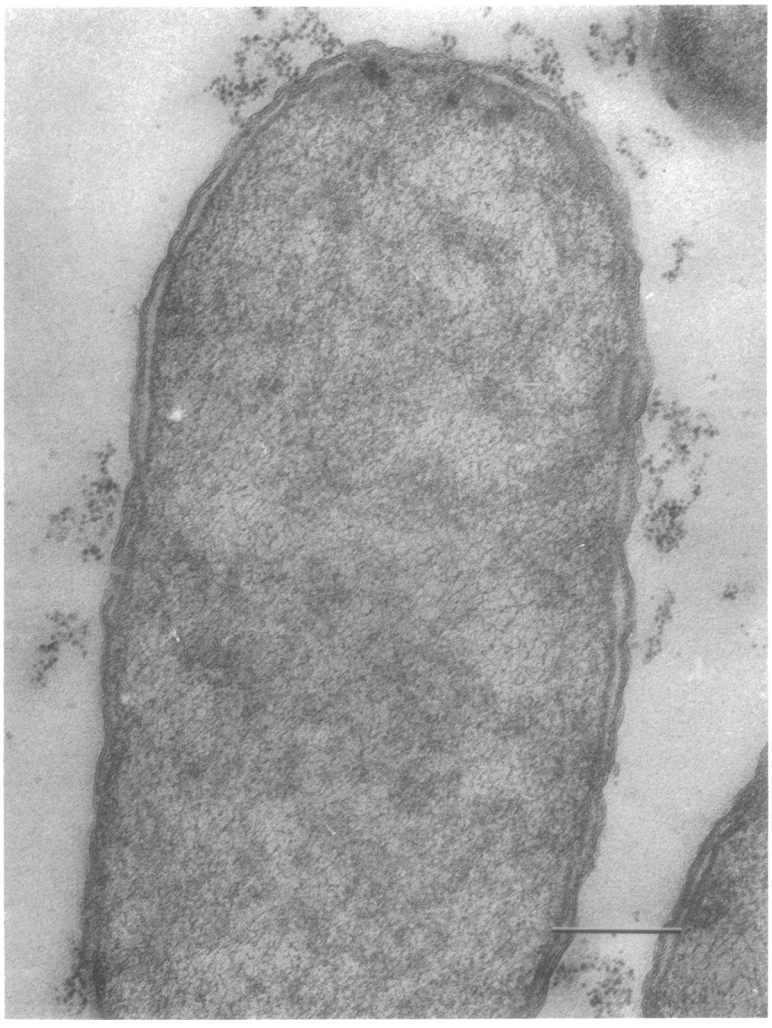

FIG. 16. *Mutant 13, 15 min after temperature shift down from 42 to 25°C. Some capsular antigen had been produced and can be localized by the ferritin IgG conjugate. Note the ferritin-labeled filaments and clusters and the multiple areas of production of the K29 polysaccharide.*

of the receding ice may suggest that in more deeply etched cells, which reveal comparatively little capsular material, the capsule has been etched away or has collapsed due to sublimation of the supporting ice. Such a rugged, spiny surface might also be generated or enhanced by a plastic deformation of the polymer during the cleavage process, a mechanism which has been suggested for intramembraneous proteins (41), polystyrol-latex, and various cell organelles (10). At present we are unable to determine whether the capsule has indeed a somewhat spiny or a very smooth surface. Furthermore, one might expect that the surface contour of the gellike capsule of *E. coli* might be uneven due to Brownian motion. Light microscopy with India ink revealed the capsule as a relatively thick organelle efficiently excluding the carbon particles of the ink; occasionally, however, single carbon particles appeared to penetrate, momentarily, deep into the capsular halo and to be expelled shortly thereafter, as if the capsule exerted some elasticity or repulsive capacity. The assumption of a continually changing surface would allow for the passing existence of deeper invaginations in the capsular contour, without lending support to the notion of preexisting holes or pores in the capsule (56). A capsule in its native state may therefore be envisaged as a very flexible, pliable, almost

TABLE 2. *Measurement of onset of production of K29 antigen in mutant 13 after temperature shift: immune reactions*

| Immune reaction | Production of K29 antigen | | | | | | | |
|---|---|---|---|---|---|---|---|---|
| | 0-1[a] | 5-10 | 15-20 | 30 | 60 | 90 | 120 | 180 |
| Slide agglutination | | | | | | | | |
| With anti-K29 IgG read after: | | | | | | | | |
| 1 min | –[b] | – | – | – | ++[c] | – | +++[d] | +++ |
| 2 min | – | 0 | (+)[e,f] | – | ++ | – | +++ | +++ |
| Tube agglutination | | | | | | | | |
| Read after 12 h | – | 0 | + | + | ++ | +++ | – | +++ |
| Electron microscopy | | | | | | | | |
| Ferritin-conjugated anti-K IgG visible on cell surface | 0 | (+) | +++ | +++ | +++ | – | – | – |
| K phage 29 adsorbed to cell surface (thin sections) | 0 | 0 | (+) | + | – | – | – | – |

[a] Minutes elapsed after shift down of cells from 46 to 25°C.
[b] –, Not measured.
[c] ++, Strong agglutination, visible within 2 min.
[d] +++, Strong agglutination, visible within 1 min.
[e] Parentheses indicate very weak reaction, only visible after agglutination time beyond 2 min.
[f] +, Weak agglutination, visible within 2 min.

TABLE 3. *Measurement of onset of production of K29 antigen in mutant 13 after temperature shift: K phage 29 receptor*

| K phage 29 receptor | Time[a] | | | | | | | |
|---|---|---|---|---|---|---|---|---|
| | 0-1 | 5-10 | 15-20 | 30 | 60 | 90 | 120 | 180 |
| K phage 29 adsorbed[b] | | | | | | | | |
| Expt | | | | | | | | |
| 1 | 0[c] | –[d] | – | 0 | 35 | 17 | 52 | – |
| 2 | 0 | – | – | – | 39 | 56 | 67 | 86 |
| 3 | – | – | – | 0 | 28 | 28 | 43 | 95 |
| 4 | 0 | 0 | 15 | 50 | 15 | 18 | 69 | 92 |
| 5 | 0 | – | 20 | 20 | 1 | 45 | – | – |

[a] Minutes elapsed after shift down of cells from 46 to 25°C.
[b] Percentage of adsorbed K phage 29 (10 min of adsorption at 0°C; multiplicity of infection, 0.1).
[c] For the controls, cells were shifted from 46 to 0°C (without growth at 25°C).
[d] –, Not measured.

liquid entity, with its contours rapidly changing and fluctuating, due to the thermal random movement of the molecules of its environment.

Capsule-specific antibody apparently cross-links the polysaccharide molecules and adds drastically to the ridigity of the resulting structure, and this occurs in direct proportion to the concentration of antibody, with an upper limit of about 0.5 mg of IgG per ml. Nonspecific antibody does not lead to such a stabilization. The smoothness of the cross-fractured capsule after exposure to anti-K29 IgG is probably the result of a size-averaging process of "cementing" the polysaccharide molecules together, which would include strands that had protruded relatively far into the medium.

Our data also indicate that the IgG molecule is able to penetrate the entire capsule, since we find an apparently homogeneous matrix in cross sections as well as in cross fractures. Further evidence for a complete and rapid penetration of the *E. coli* capsule is derived from the fact that capsule-specific bacteriophage 29, which penetrates the capsule in less than 1

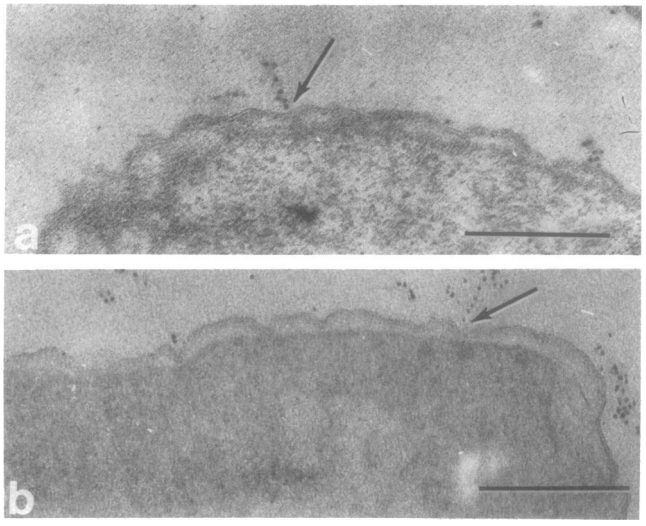


FIG. 17. *The immune-reactive filaments (a and b) seem often to protrude from areas of wall-membrane adhesion (arrows).*

min, can be stopped "mid-way" in its penetration by simultaneous addition of anti-capsule IgG. This would indicate a relatively fast penetration of the IgG molecule into the deeper regions of the capsule (Bayer and Thurow, manuscript in preparation).

Furthermore, our data demonstrate ultrastructural aspects of the "quellungs reaction" of capsules after antibody treatment. This reaction was described for fungi and pneumococci many years ago, and it was proposed as a diagnostic tool for detection of capsular antigens (46). The chemical structure of the capsular polysaccharide has been largely elucidated by employment of capsule-degrading bacteriophages (37, 57–61). The serotype K29 polysaccharide is degraded by the K-specific phage 29 (17), similar to the degradation of *Klebsiella* polysaccharides by phages 11, 20, and 24 (5, 62). We have shown that during infection of the cells, phage 29 leaves a tunnel-like path in the capsule (Bayer and Thurow, manuscript in preparation). Chemical analysis suggested that the capsules of gram-negative bacteria consist of fibrillar molecules (23). The K29 polysaccharide-consists of about 300 hexasaccharide-repeating units with a backbone of mannose, glucose, glucuronic acid, and galactose in a 1:1:1:1 ratio (9, 47). At the glucuronic acid, a side chain of mannose, glucose, and pyruvate is attached. Repeating subunits similar to this were reported for many of the linear polymers of capsules and slimes; their molecular weights are $10^5$ and higher (39, 47).

Filamentous forms of K-antigens were described for *E. coli* K88 and K99, which are both virulent strains (6, 60). Their virulence appears to be associated with the presence of the filamentous antigens, enabling the bacteria to adhere and to colonize to the mucosa of the small intenstine of pigs and calves, respectively, suffering from neonatal diarrhea (6). In the microscope, however, one observes clearly individual filaments protruding into the environment of the cells; thus, these antigens seem to be of much less quantitiy or area density than the K29 polysaccharides.

It has been shown by Nhan et al. (47), Choy et al. (9), and others, that alkali treatment abolishes the heterogeneity in the sedimentation profiles of the capsular polysaccharides, possibly by breaking bonds between neighboring chain molecules; this treatment has no effect on sugar content or on the serological activity of the resulting material. We observed that NaOH treatment of the polysaccharide affected the length and thickness of the filamentous bundles, causing also a decrease in the viscosity of the polymer (data not shown). After 4 h of exposure to alkali, a group of thin fibers of 250- to 350-nm length became abundantly visible. The thin fiber might represent a major subunit class of the K29 polysaccharide. Estimates of the molecular weight of these filaments can only be very rough, due to the unknown contribution to the thickness of the cytochrome *c* film and the platinum shadowcast. The molecular weight of such a fiber would range from $10^7$ to almost $10^8$ representing a multiple of the estimated molecular weight of the K29 polymer

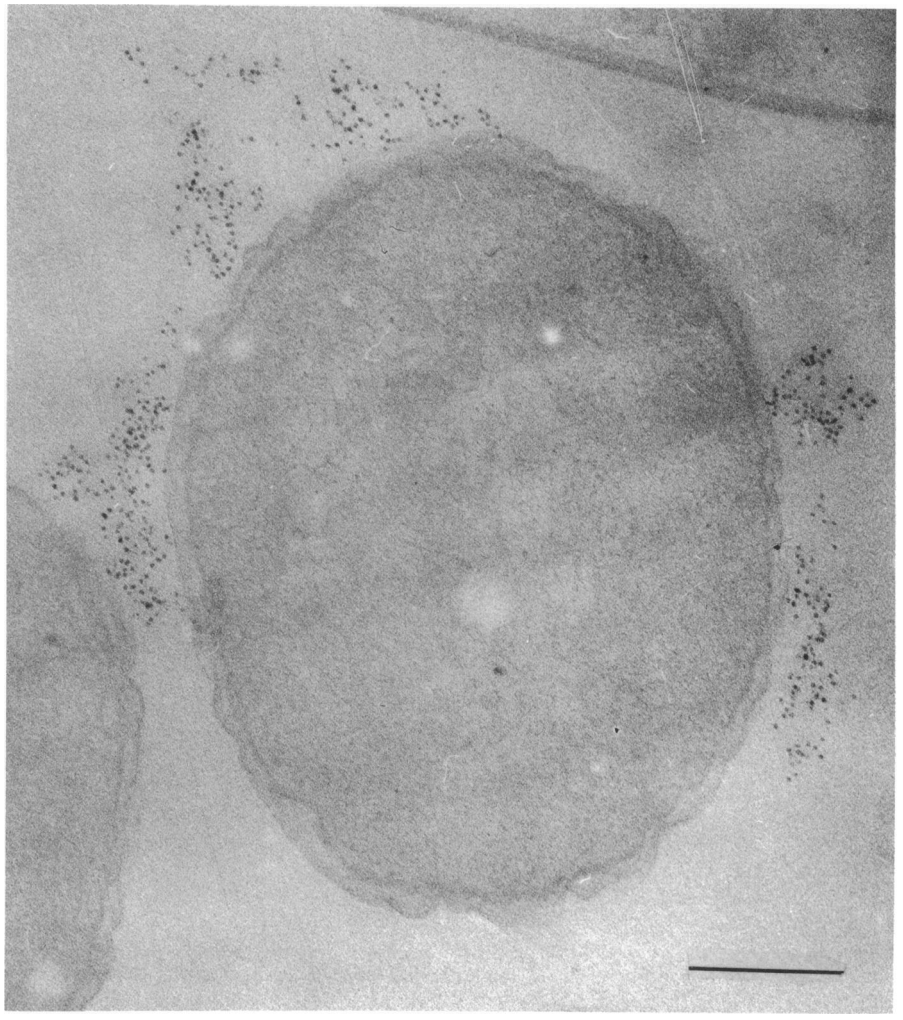

FIG. 18. *Twenty-five minutes after growth at permissive temperature, the ferritin-IgG complex depicts large cloudlike arrangements of the capsular material.*

(38, 47). The polysaccharide fibers appear to be unbranched and of lesser complexity than glycoproteins from articular cartilage (52) and proteoglycan molecules from phenol extracts of mitochondrial deoxyribonucleic acid (63), which reveal a backbone with side branches. A reticulate association of molecules was observed for pectin (22) that resembled (morphologically) a state similar to that of the K29 polysaccharide before NaOH treatment.

The composition and the role of the knoblike element visible at one end of most of these filaments is now known; it might be a coiled portion of the filamentous molecule, or it might be involved in anchoring the filament within the outer membrane. We tested, without success, for LPS antigenicity by Ouchterlony gel diffusion, by immunoelectrophoresis, and by reacting the APS with ferritin-conjugated anti-O IgG.

Although it appears from our data that the export sites of newly synthesized capsule polysaccharide are located at the sites of adhesion of inner and outer membrane, the fate of the "older" polysaccharide molecule remains a matter of speculation: the molecule might be diffusing along the cell surface, or the sites of synthesis might be shifted to new, nearby sites "seeding" the entire surface with bundles of polysaccharide.

The thickness of the antibody-treated capsule measured 250 to 350 nm in freeze-etchings.

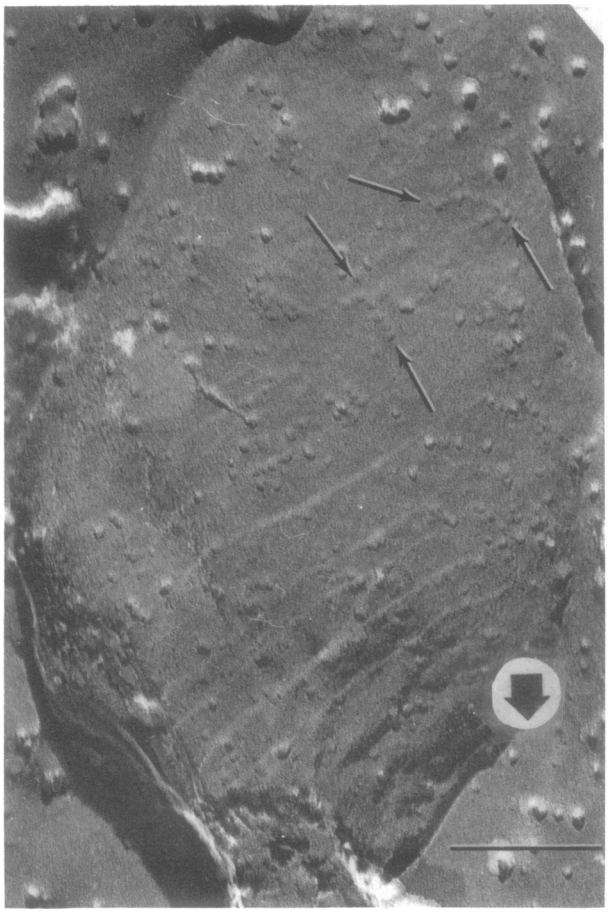

FIG. 19. *Analogous to the thin sections (Fig. 16), freeze-etched cell surfaces show the newly formed antigen by revealing the ferritin of the anti-K29 conjugate; the two aspects of the antigen can be seen, the filaments (arrows) and the clusters. (Broad arrow indicates direction of shadowing as in Fig. 7 through 9.)*

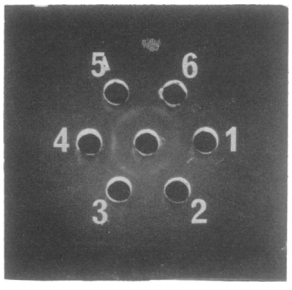


FIG. 20. *Immunodiffusion in agarose gel; anti-K29 IgG in the center well and polysaccharides of K29 (1 and 2), M13 (3 and 4), and M41 (5 and 6) in the periphery. The polysaccharides are shown before (1, 3, and 5) and after (4 h) alkali treatment (2, 4, and 6).*

Some of the ultrathin sections suggest (see Fig. 11) fibrous elements in an orientation more or less normal to the cell surface. For such an arrangement, the length of the APS fiber of about 300-nm length would be sufficient to extend from the outer membrane of the envelope through the entire width of the capsule.

In contrast to the wild type, mutants such as M41 and M13 produce at permissive temperatures a "stringy" polysaccharide that forms, at the cell surface, either long filaments or coiled configurations (see Fig. 15 to 18). The length of these polysaccharide strands does not seem to be stringently regulated. Although the mutant colonies showed the characteristics of slime-producing cells, we have demonstrated their common K29 antigenicity by immunodiffusion, as well as their sensitivity to phage K29. We have not excluded the presence of minor amounts of additional components in the polysaccharide such as, for example, colanic acid (21). However, recently we were able to obtain X-ray diffraction data of crystalline fibers of the polysaccharides of mutants 13 and 41, as well as

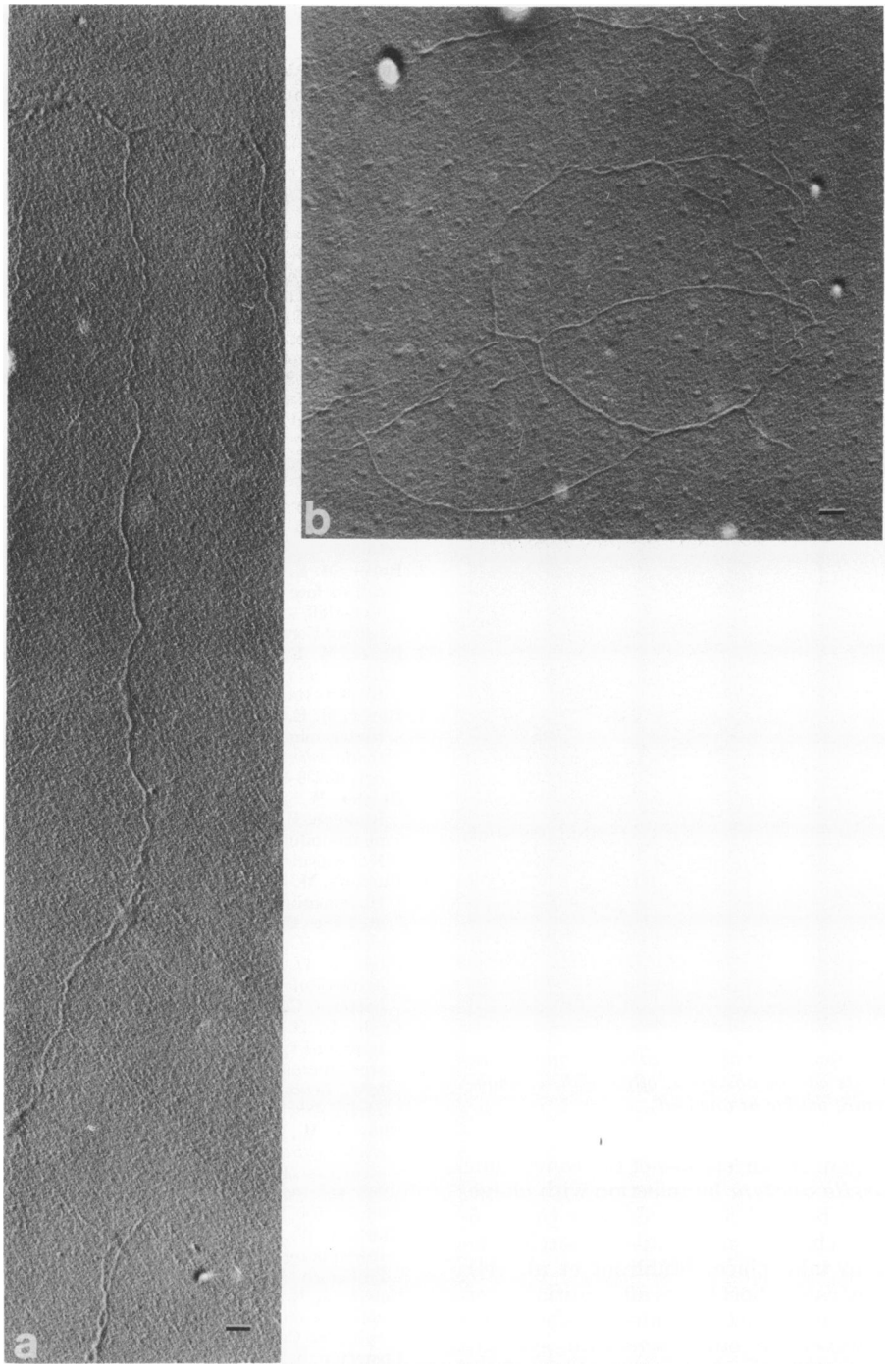


FIG. 21. *After spreading the isolated capsular polysaccharide on water-air interfaces, one observes (a) filamentous structures of varying thickness and (b) entangled loops plus free ends. (The white circular areas in the background are holes in the supporting membrane.)*

from the wild-type K29, and from these it appears that no additional major component is present in the polysaccharide of the mutants (42a).

The time required for export of K-antigen is considerably longer in the mutant 13 than the time needed for emergence of another surface component of gram-negative bacteria, namely

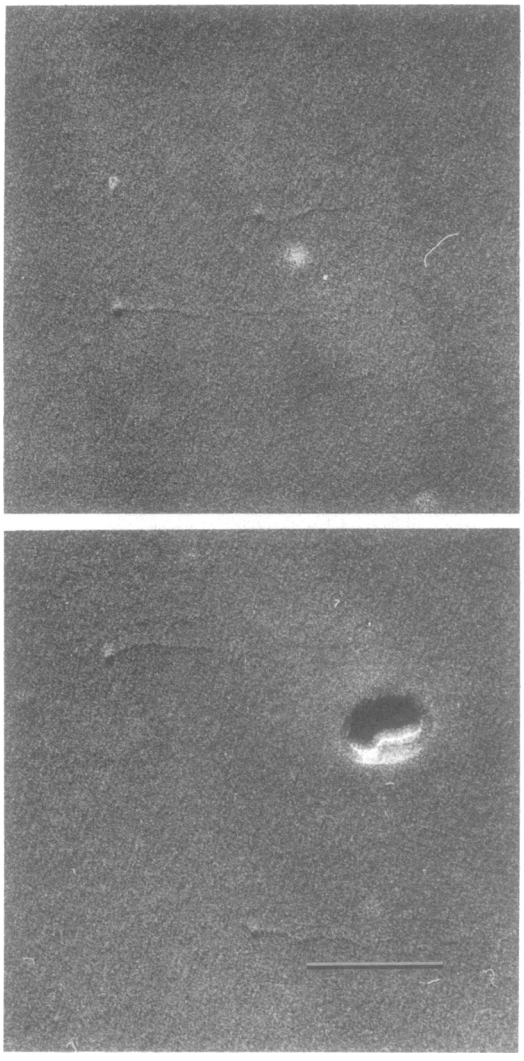

FIG. 22. *After 4 h of alkali treatment, many delicate filaments can be observed, often with a "knob-like" structure visible at one end.*

the O-antigen. In our studies of the conversion in *Salmonella anatum* by infection with phage $\epsilon$15 (2), we observed as the shortest time 1.5 min for the changes of the lipopolysaccharide structure to take place. Mühlradt et al. (44) found comparably short times after initiation of LPS export in galactose-epimerase-less mutants. However, in our *Salmonella* system, these short times were only attainable in fast-growing cells, i.e., in cultures with generation times of around 18 min. In comparison, at 46°C the generation times of our *E. coli* mutant 13 is more than 2 h; after shift down to 25°C, it diminishes to a generation time of 50 min over the first hour. Thus, the slower growth rate of the mutant might be paralleled by a slower production rate of the capsular antigen. In addition, the mutation step might also have directly affected mechanisms and rates of synthesis of this cell surface component.


## ACKNOWLEDGMENTS

This investigation was supported by Public Health Service grant AI-10414 from the National Institute of Allergy and Infectious Diseases and National Science Foundation grant BMS73-01121 to M. E. B. as well as Public Health Service grants CA-06927 and RR-05539 from the National Cancer Institute; we also received appropriation from the Commonwealth of Pennsylvania.

We thank E. Starkey, J. Fink, and B. Dupree for their able technical assistance, and B. Janaitis for the execution of the secretarial work.


## LITERATURE CITED


1. **Bayer, M. E.** 1968. Areas of adhesion between wall and membrane of *Escherichia coli*. J. Gen. Microbiol. 53:395-404.
2. **Bayer, M. E.** 1975. Role of adhesion zones in bacterial cell surface function and biogenesis, p. 393-427. *In* A. Tzagaloff (ed.), Membrane biogenesis. Plenum Publishing Corp., New York.
3. **Bayer, M. E., and C. C. Remsen.** 1970. Structure of *Escherichia coli* after freeze-etching. J. Bacteriol. 101:304-314.
4. **Bayer, M. E., and T. Starkey.** 1972. The adsorption of bacteriophage ΦX174 and its interaction with *Escherichia coli:* a kinetic and morphological study. Virology 49:236-256.
5. **Bessler, W., E. Freund-Mölbert, H. Knufermann, C. Rudolph, H. Thurow, and S. Stirm.** 1973. A bacteriophage-induced depolymerase active on Klebsiella K11 capsular polysaccharide. Virology 56:134-151.
6. **Burrows, M. R., R. Sellwood, and R. A. Gibbons.** 1976. Haemagglutinating and adhesive properties associated with the K99 antigen of bovine strains of *Escherichia coli*. J. Gen. Microbiol. 96:269-275.
7. **Cagle, G. D.** 1975. Fine structure and distribution of extracellular polymer surrounding selected anerobic bacteria. Can. J. Micribiol. 21:395-408.
8. **Cagle, G. D., R. M. Pfister, and G. R. Vela.** 1972. Improved staining of extracellular polymer for electron microscopy: examination of *Azobacteria, Zoogloea, Leuconostoc,* and *Bacillus*. Appl. Microbiol. 24:477-488.
9. **Choy, Y.-M., F. Fehmel, N. Frank, and S. Stirm.** 1975. *Escherichia coli* capsule bacteriophages. VI. Primary structure of the bacteriophage 29 receptors, the *E. coli* serotype 29 capsular polysaccharide. J. Virol. 16:581-590.
10. **Clark, A. W., and D. Branton.** 1968. Fracture faces in frozen outer segments from the guinea pig retina. Z. Zellforsch. Mikrosk. Anat. 91:586-603.
11. **Colvin, J. R., and M. Beer.** 1960. The formation of cellulose microfibroids in suspensions of Acetobacter xylinum. Can. J. Microbiol. 6:631-637.
12. **Costerton, J. W., H. N. Damgaard, and K. J. Cheng.** 1974. Cell envelope morphology of rumen bacteria. J. Bacteriol. 118:1132-1143.
13. **Cota-Robles, E.** 1963. Electron microscopy of plasmolysis in *Escherichia* J. Bacteriol. 85:499-503.
14. **Creech, H. J., R. K. Preston, R. M. Peck, and A. P. O'Connell.** 1972. Anti-tumor and mutagenic properties of a variety of hetero-cyclic nitrogen and sulfur

mustards. J. Med. Chem. 15:739–746.
15. **Draper, P., and R. J. W. Rees.** 1973. The nature of the electron transparent zone that surrounds mycobacterium lepraemurium inside host cells. J. Gen. Microbiol. 77:79–87.
16. **Dubois, M., K. A. Gilles, J. K. Hamilton, P. Rebers, and F. Smith.** 1956. Colorimetric method for determination of sugars and related substances. Anal. Chem. 28:350–356.
17. **Fehmel, F., U. Feige, H. Niemann, and S. Stirm.** 1975. *Escherichia coli* capsule bacteriophages. VII. Bacteriophage 29-host capsular polysaccharide interactions. J. Virol. 16:591–601.
18. **Fletcher, M., and G. D. Floodgate.** 1973. An electron microscope demonstration of an acidic polysaccharide involved in the adhesion of a marine bacterium to solid surfaces. J. Gen. Microbiol. 74:325–344.
19. **Gautier, A. R., M. Schreyer, R. Cogliati, and J. Fakanova.** 1971. "Shiff-type" - electron stains in ultrastructural cytochemistry. Experientia 27:735.
20. **Gibbons, R. J., and P. H. Keyes.** 1969. Inhibition of insoluble dextran synthesis, plaque formation and dental caries in hamsters by low molecular weight dextran. Arch. Oral Biol. 14:721–724.
21. **Grant, W. D., I. W. Sutherland, and J. F. Wilkinson.** 1969. Exopolysaccharide colanic acid and its occurrence in the *enterobacteriaceae*. J. Bacteriol. 100:1187–1193.
22. **Hanke, D. E., and D. H. Northcote.** 1975. Molecular visualization of pectin and DNA by ruthenium red. Biopolymers 14:1–17.
23. **Heidelberger, M., F. E. Kendall, and H. W. Scherp.** 1936. The specific polysaccharides of types I, II and III pneumococcus. J. Exp. Med. 64:577–584.
24. **Hsu, K. C., and S. S. Breese.** 1971. Techniques of ferritin-tagged antibodies. *In* N. Maramorosch and H. Koprowski (ed.), Methods in virology, vol. 5. Academic Press Inc., New York.
25. **Hungerer, D., K. Jann, B. Jann, F. Ørskov, and I. Ørskov.** 1967. Immunochemistry of K-antigens of *Escherichia coli*. IV. The K-antigen of *E. coli* O9:K30:H12. Eur. J. Biochem. 2:115–126.
26. **Jann, K., B. Jann, F. Ørskov, and I. Ørskov.** 1966. Immunochemische Untersuchungen and K-Antigenen von *Escherichia coli*. III. Isolierung und Untersuchung der chemischen Struktur des sauren Polysaccharids aus *E. coli* O141:K85(B):H4 (K85-Antigen). Biochem. Z. 346:368–385.
27. **Jann, K., B. Jann, F. Ørskov, I. Ørskov, and O. Westphal.** 1965. Immunchemische Untersuchungen an K-Antigenen von *Escherichia coli*. II. Das K-Antigen von *E. coli* O8:K42(A):H$^-$. Biochem. Z. 342:1–22.
28. **Jones, H. C., J. C. Roth, and W. M. Sanders.** 1969. Electron microscopic studies of a slime layer. J. Bacteriol. 99:316–325.
29. **Kaiser, G. E., and M. J. Starzyk.** 1973. Ultrastructure and cell division of an oral bacterium resembling Alysiella filiformis. Can. J. Microbiol. 19:325–327.
30. **Kauffmann, F.** 1944. Zur Serologie der Coli-Gruppe. Acta Pathol. Microbiol. Scand. 21:20–45.
31. **Kauffman, F.** 1969. The bacteriology of enterobacteriaceae. 2nd ed. The Williams and Wilkins Co., Baltimore.
32. **Kelstrup, J., and T. D. Funder-Nielsen.** 1972. Molecular interactions between the extracellular polysaccharides of streptococcus mutants. Arch. Oral Biol. 17:1659–1670.
33. **Klein, P., and W. R. Adams.** 1972. Location of ferritin-labeled concanavalin A zinding to influenza virus and tumor cell surfaces. J. Virol. 10:844–854.
34. **Kleinschmidt, A. K.** 1968. Monolayer techniques in electron microscopy of nucleic acid molecules, p. 361–379. *In* L. Crossman and K. Moldave (ed.), Methods in enzymology, vol. 12, part B. Academic Press Inc., New York.
35. **Kleinschmidt, A. K., and R. K. Zahn.** 1959. Über Desoxyribonukleinsaure Molekeln in Protein Mischfilmen. Z. Naturforsch. Teil B. 14:770–779.
36. **Labaw, L. L., and V. M. Mosley.** 1954. Demonstration of striated fibers in the capsule of the Lisbonne strain lysogenic Escherichia coli. J. Bacteriol. 67:576–584.
37. **Lindberg, A.** 1973. Bacteriophage receptors. Annu. Rev. Microbiol. 27:205–241.
38. **Lonngren, J., and A. Pilotti.** 1971. Gas liquid chromatography of partially methylated alditols as their acetates. II. Acta Chem. Scand. 25:1144–1145.
39. **Lüderitz, O., K. Jann, and R. Wheat.** 1968. Somatic and capsular antigens of gram-negative bacteria. Compr. Biochem. 26A:105–228.
40. **Luft, J. H.** 1966. Ruthenium red staining of the striated muscle cell membrane and the myotendinal junction. Proc. 6th Int. Congr. Electron Microsc. Jpn. 2:65.
41. **Meyer, H. W., and H. Winkelmann.** 1972. Über die Anordnung der Membran-proteine nach Untersuchungen mit der Gefrierätzung an isolierten Erythrozytenmembranen. Protoplasma 75:255–284.
42. **Mollenhauer, H. H.** 1964. Plastic embedding mixtures for use in electron microscopy. Stain Technol. 39:11–49.
42a. **Moorhouse, R., W. T. Winter, S. Arnott, and M. E. Bayer.** 1977. Conformation and molecular organization of fibers of the capsular polysaccharide from *Escherichia coli* M41 mutant. J. Mol. Biol. 109: 373–391.
43. **Mudd, S., F. Heinmets, and T. F. Anderson.** 1943. The pneumococcal capsular swelling reaction, studied with the aid of the electron microscopy. J. Exp. Med. 78:327–332.
44. **Mühlradt, P., J. Menzel, J. R. Golecki, and V. Speth.** 1973. Outer membrane of Salmonella. Sites of export of newly synthesized lipopolysaccharide on the bacterial surface. Eur. J. Biochem. 35:471–481.
45. **Nanninga, N.** 1970. Ultrastructure of the cell envelope of *Escherichia coli* B after freeze-etching. J. Bacteriol. 101:297–303.
46. **Neufeld, F.** 1902. Ueber die Agglutination der Pneumokokken und über die Theorieen der Agglutination. Z. für Infektionskrankheiten. Parasitäre Krankheiten und Hygiene der Haustiere 40:54–72.
47. **Nhan, L. B., B. Jann, and K. Jann.** 1971. Immunochemistry of K-antigens of *Escherichia coli* O9:K29(A):H$^-$. Eur. J. Biochem. 21:226–234.
48. **Ørskov, I., F. Ørskov, B. Jann, and K. Jann.** 1963. Acidic polysaccharide antigens of a new type from *E. coli* capsules. Nature (London) 200:144–146.
49. **Ouchterlony, O.** 1958. Diffusion-in-gel methods for immunological analysis. Prog. Allergy 5:1–43.
50. **Reynolds, E. S.** 1963. The use of lead citrate at high pH as an electron spaque stain in electron microscopy. J. Cell. Biol. 17:208–212.
51. **Roger, D. H.** 1896. Les Infections non Bacteriénnes. Rev. Gen. Sci. Appl. 7:770–775.
52. **Rosenberg, L., W. Hellmann, and A. Kleinschmidt.** 1975. Electron microscopic studies of proteoglycan aggregates from bovine articular cartilage. J. Biol. Chem. 250:1877–1883.
53. **Schmidt, G.** 1972. Basalstrukturen von Lipopolysachariden verschiedener Enterobacteriaceen. Genetische und serologische Untersuchungen an R-Mutaten. Zentralbl. Bakteriol. Parasitenkd. Infektionskr. Hyg. Abt. 1: Orig. Reihe A A220:472–476.
54. **Scott, J. E.** 1960. Aliphatic ammonium salts in the assay of acidic polysaccharides from tissues. Methods Biochem. Anal. 8:145–197.
55. **Springer, L., and I. L. Roth.** 1973a. The ultrastructure of the capsules of Diplococcus pneumoniae and Kleb-

siella penumoniae stained with ruthenium red. J. Gen. Microbiol. 74:21–31.
56. **Springer, L., and I. L. Roth.** 1973b. Ultrastructure of the capsule of Klebsiella pneumoniae and slime of Enterobacter aerogenes revealed by freeze-etching. Arch. Mikrobiol. 93:277–286.
57. **Stirm, S., W. Bessler, F. Fehmel, and E. Freund-Mölbert.** 1971. Bacteriophage particles with endoglycosidase activity. J. Virol. 8:343–346.
58. **Stirm, S., W. Bessler, F. Fehmel, E. Freund-Mölbert, and H. Thurow.** 1971. Isolation of spike-formed particles from bacteriophage lysates. Virology 45:303–308.
59. **Stirm, S., and E. Freund-Mölbert.** 1971. *Escherichia coli* capsule bacteriophages. II. Morphology. J. Virol. 8:330–342.
60. **Stirm, S., F. Ørskov, I. Ørskov, and A. Birch-Andersen.** 1967. Episome-carried surface antigen K88 of *Escherichia coli*. III. Morphology. J. Bacteriol. 93:740–748.
61. **Taylor, K.** 1966. Physical and chemical changes of Vi-polysaccharide due to Vi-phage II action. Acta Biochim. Pol. 13:97–106.
62. **Thurow, H., H. Niemann, C. Rudolph, and S. Stirm.** 1974. Host capsule depolymerase activity of bacteriophage particles active on Klebsiella K 20 and K 24 strains. Virology 58:306–309.
63. **Wellauer, P., and R. Weber.** 1971. A structure resembling proteinpolysaccharide complexes in preparations of mitochondrial DNA from mouse liver. Experientia 27:1171–1173.
64. **Westphal, O., and K. Jann.** 1965. Bacterial lipopolysaccharides. Extraction with phenol-water and further applications of the procedure, p. 83–91. *In* R. L. Whistler (ed.). Methods in carbohydrate chemistry, vol. 5. Academic Press Inc. New York and London.
65. **Wilkinson, J. F.** 1958. The extracellular polysaccharides of bacteria. Bacteriol. Rev. 22:46–73.
66. **Wilkinson, J. F., J. P. Duguid, and P. N. Edmunds.** 1954. The distribution of polysaccharide production in Aerobacter and Escherichia strains and its relation to antigenic characters. J. Gen. Microbiol. 11:59–72.